

## 2-Ethyl and 2-Ethylidene Analogues of 1 $\alpha$ ,25-Dihydroxy-19-norvitamin D<sub>3</sub>: Synthesis, Conformational Analysis, Biological Activities, and Docking to the Modeled rVDR Ligand Binding Domain

Rafal R. Sicinski,<sup>†,§</sup> Piotr Rotkiewicz,<sup>‡</sup> Andrzej Kolinski,<sup>‡</sup> Wanda Sicinska,<sup>†</sup> Jean M. Prahl,<sup>†</sup> Connie M. Smith,<sup>†</sup> and Hector F. DeLuca<sup>\*,†</sup>

Department of Biochemistry, University of Wisconsin–Madison, 433 Babcock Drive, Madison, Wisconsin 53706, and Department of Chemistry, University of Warsaw, Pasteura 1, 02-093 Warsaw, Poland

Received January 7, 2002

Novel 19-nor analogues of 1 $\alpha$ ,25-dihydroxyvitamin D<sub>3</sub> were prepared and substituted at C-2 with an ethylidene group. The synthetic pathway was via Wittig–Horner coupling of the corresponding A-ring phosphine oxides with the protected 25-hydroxy Grundmann's ketones. Selective catalytic hydrogenation of 2-ethylidene analogues provided the 2 $\alpha$ - and 2 $\beta$ -ethyl compounds. The 2-ethylidene-19-nor compounds with a methyl group from the ethylidene moiety in a trans relationship to the C(6)–C(7) bond (*E*-isomers) were more potent than the corresponding *Z*-isomers and the natural hormone in binding to the vitamin D receptor. Both geometrical isomers (*E* and *Z*) of (20*S*)-2-ethylidene-19-norvitamin D<sub>3</sub> and both 2 $\alpha$ -ethyl-19-norvitamins (in the 20*R*- and 20*S*-series) have much higher HL-60 differentiation activity than does 1 $\alpha$ ,25-(OH)<sub>2</sub>D<sub>3</sub>. Both *E*-isomers (20*R* and 20*S*) of 2-ethylidene vitamins are characterized by very high calcemic activity in rats. The three-dimensional structure model of the rat vitamin D receptor and the computational docking of four synthesized (20*R*)-19-norvitamin D<sub>3</sub> analogues into its binding pocket are also reported.

### Introduction

The discovery of the hormonally active form of vitamin D<sub>3</sub>, 1 $\alpha$ ,25-dihydroxyvitamin D<sub>3</sub> (1 $\alpha$ ,25-(OH)<sub>2</sub>D<sub>3</sub>, calcitriol, **1**, Figure 1), has greatly stimulated research into its physiology and chemistry.<sup>1,2</sup> It has been established that **1** not only regulates the mineral metabolism in animals and humans<sup>3</sup> but also affects the human immune system and exerts potent effects upon cell proliferation and cellular differentiation.<sup>4</sup> Therefore, the study of the chemistry of vitamin D has been recently focused on the design and synthesis of such analogues which can exert selective biological actions.<sup>5</sup> In our continuing investigation of the structure–activity relationship of the vitamin D molecule, we prepared an analogue of the natural hormone **1**, 1 $\alpha$ ,25-dihydroxy-2-methylene-19-norvitamin D<sub>3</sub> (**2a**),<sup>6</sup> in which the exocyclic methylene group is transposed, in comparison with **1**, from C-10 to C-2. Also, the 2 $\alpha$ -methyl analogue **4a** was obtained by a selective hydrogenation of **2**. Both analogues, being formally derivatives of 19-nor-1 $\alpha$ ,25-(OH)<sub>2</sub>D<sub>3</sub> (**3a**) synthesized by us previously,<sup>7</sup> were characterized by significant biological potency, enhanced especially in their isomers in the 20*S*-series (**2b**, **4b**).<sup>6</sup> As a continuation of our search for biologically active vitamin D compounds possessing A-ring conformational equilibrium shifted to one particular chair form, we prepared novel 19-nor analogues of **1** substituted at C-2

with ethyl (**6a,b** and **7a,b**) and ethylidene (**8a,b** and **9a,b**) groups. We also performed docking molecular simulations with the four vitamins from the 20*R*-series (**6a–9a**) using the computational model of the full-length ligand binding domain of the rat vitamin D receptor (rVDR-LBD).

### Results and Discussion

**Chemistry.** The strategy of synthesis was based on the Lythgoe-type Wittig–Horner coupling approach<sup>8</sup> which was successfully used by us in the preparation of other 2-substituted 19-norvitamins.<sup>6,9</sup> Availability of the corresponding protected 25-hydroxy Grundmann's ketones with “natural” (**19a**)<sup>9</sup> and inverted (**19b**)<sup>6</sup> configurations at C-20 directed our attention to the preparation of the phosphine oxide A-ring synthons **17** and **18** (Scheme 1).

The hydroxycyclohexanone compound **10** was synthesized in 4 steps (25% yield) from commercially available (1*R*,3*R*,4*S*,5*R*)-(–)-quinic acid.<sup>10</sup> Catalytic oxidation with ruthenium tetroxide afforded cyclohexanedione derivative **11** in 65% yield. Due to a considerable difference in the steric hindrance between the two carbonyl groups, it was possible to achieve selective Peterson olefination with methyl(trimethylsilyl)acetate providing allylic ester **12** in 67% yield. However, the following Wittig reaction with a ylide generated from ethyltriphenylphosphonium bromide and *n*-BuLi proved to be much less efficient. Our attempts to improve the yield (18%) by changing reaction conditions and bases used for the ylide preparation (for example, potassium and sodium bis(trimethylsilyl)amides) were not successful. The <sup>1</sup>H NMR spectrum of the resulting mixture of 4'-ethylidene compounds **13** and **14** indicated a presence of two

\* To whom correspondence should be addressed: Department of Biochemistry, University of Wisconsin–Madison, 433 Babcock Drive, Madison, WI 53706. Telephone: 608-262-1620. Fax: 608-262-7122. E-mail: deluca@biochem.wisc.edu.

<sup>†</sup> University of Wisconsin–Madison.

<sup>‡</sup> University of Warsaw.

<sup>§</sup> Present address: Department of Chemistry, University of Warsaw, ul. Pasteura 1, 02-093 Warsaw, Poland.

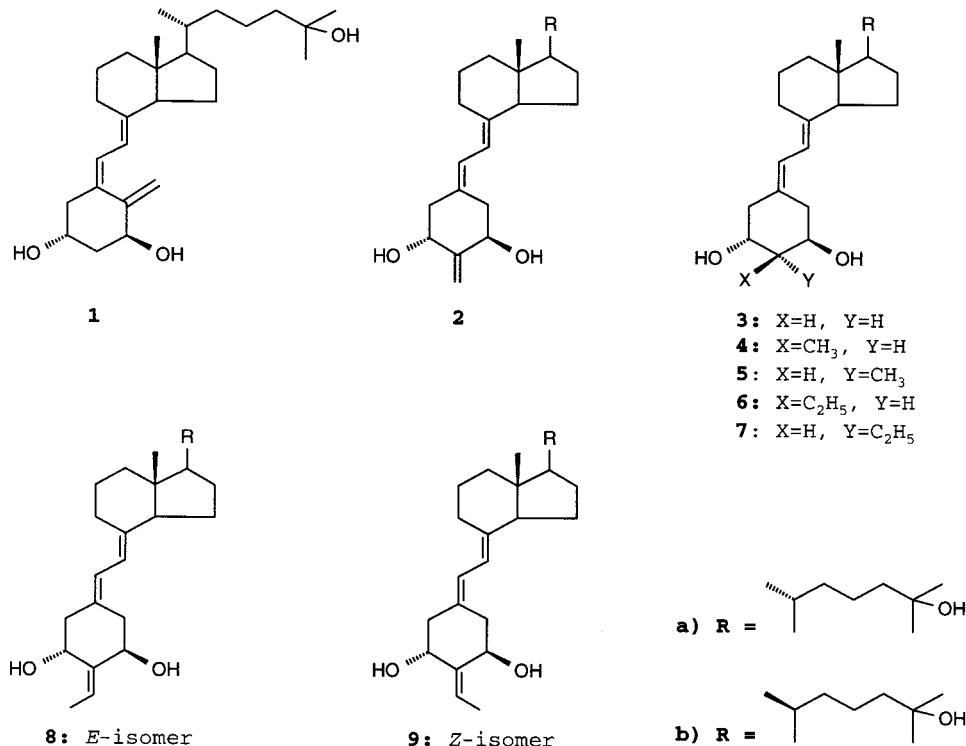


**Figure 1.** Chemical structure of 1 $\alpha$ ,25-dihydroxyvitamin D<sub>3</sub> (calcitriol, **1**) and its analogues.

geometrical isomers (1:1.7 ratio) differing in the orientation of a carbomethoxy group and a methyl group from the ethylidene moiety (both groups are considered substituents of terminal carbon atoms in a 1,4-dimethylenecyclohexane fragment). Although the spectrum was characterized by good proton dispersion, the assignment of their structures was performed after the following DIBALH reduction step due to difficulties with chromatographic separation of the isomers. Allylic alcohols **15** and **16** (80% yield) were easily separated by preparative HPLC, and their configurations as well as preferred conformations were unequivocally established by <sup>1</sup>H NOE difference spectroscopy and spin decoupling experiments. Analysis of the proton coupling network supported the expected strong preference of chair conformers possessing an axial orientation of this OTBDMS group to which the methyl group from 4'-ethylidene moiety is directed. For example, in the major isomer (Figure 2b), a signal of an equatorial proton at C-6' ( $\delta$  2.50) was assigned by a NOE experiment involving vinylic 2-H ( $\delta$  5.73). The coupling constant of its geminal partner resonating at  $\delta$  2.02 with the vicinal proton at C-5' (ca. 11 Hz) is typical for protons in axial/axial orientation and clearly indicates a significant bias toward one chair-like cyclohexane ring conformation with the 3'- and 5'-OTBDMS groups in axial and equatorial orientation, respectively. Two NOE experiments involving the irradiation of axial 5' $\alpha$ -H and equatorial 3' $\beta$ -H show a 2.6% enhancement of a vinylic proton ( $\delta$  5.59) from the ethylidene unit and a 12.2% enhancement of the methyl signal ( $\delta$  1.70), respectively, supporting a *Z* relationship of the latter with the 1-hydroxymethyl group (**16**). The coupling constants and the observed NOEs in the minor isomer presented in Figure 2a demonstrate that the methyl substituent of the ethylidene moiety is in close proximity to the

equatorial proton at C-5' and, therefore, in *E* relationship to 1-CH<sub>2</sub>OH (**15**). Each of the isomeric allylic alcohols **15** and **16** was then transformed to the desired A-ring phosphine oxide synthons **17** and **18** using an efficient (ca. 60%) three-step procedure of tosylation, reaction with a diphenylphosphine anion, and oxidation with hydrogen peroxide. The subsequent Wittig–Horner reaction of the conjugate base of **17** with the protected 25-hydroxy Grundmann's ketone **19a** produced 19-norvitamin D<sub>3</sub> compound **20a** in excellent yield (91%), but the yield of an analogous coupling of the isomeric phosphine oxide **18** was very low (13%).

A striking difference in the reactivity of the isomeric phosphine oxides in Wittig–Horner coupling with **19a** was nicely demonstrated when the 1:2 mixture of **17** and **18** was used. This resulted in the formation of practically pure 19-norvitamin D<sub>3</sub> compound **20a** derived from the minor *E*-isomer! A possible explanation of this intriguing observation can be obtained from the consideration of a steric hindrance in the corresponding intermediates formed in the first step of the Wittig–Horner reaction. Most likely, an attack of the lithium phosphinoxy carbanion, produced from **18** and *n*-BuLi, on C-8 takes place from the  $\alpha$ -side of the Grundmann's ketone molecule and results in the 8 $\beta$ -hydroxy adduct. The configuration of the ethylidene substituent forces the 1 $\alpha$ -OTBDMS group to adopt an axial orientation, and this bulky substituent, interacting with substituents of the phosphorus atom, restricts rotation around the C(7)–C(8) bond, destabilizing the *syn*-periplanar conformation of the P–C(7)–C(8)–O fragment (Figure 3) required for a *syn*-elimination of diphenylphosphinic acid<sup>11,12</sup> and the formation of a 7*E*-double bond. On the basis of the literature data indicating reversibility of the first step of Wittig reactions involving phosphine oxides,<sup>11</sup> the low yield of the diene

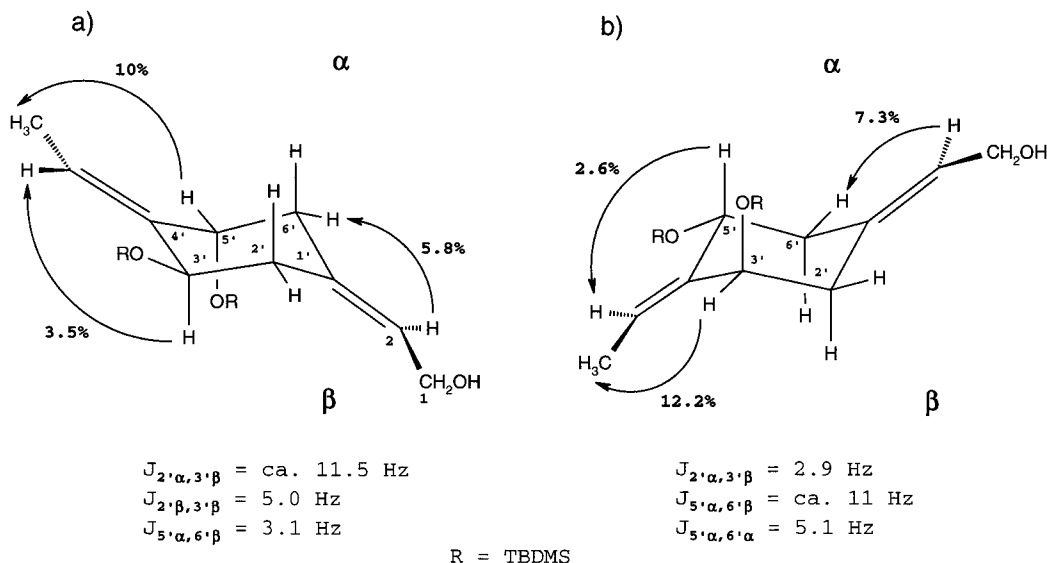
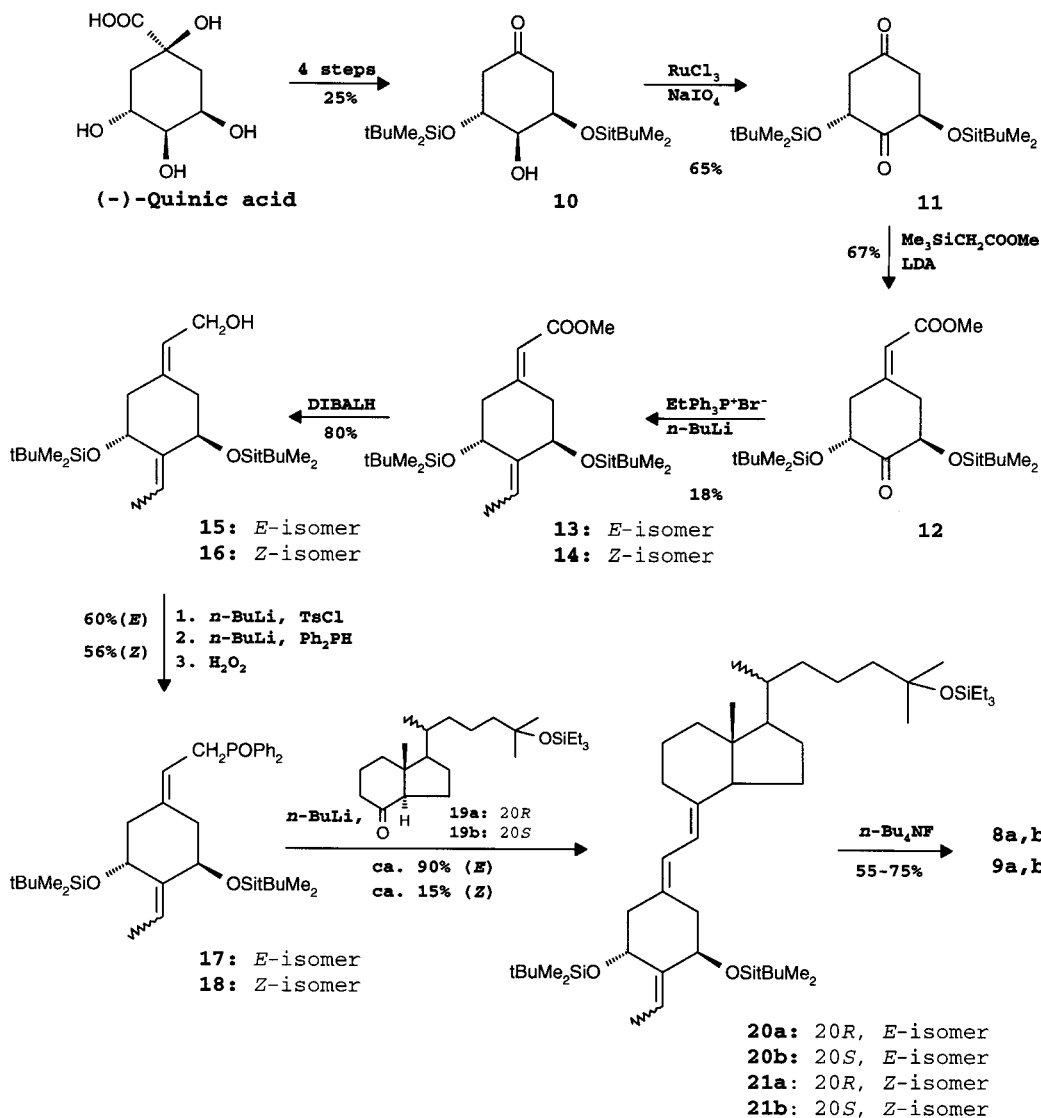


**Figure 2.** Preferred conformations of the synthesized allylic alcohols **15** (a) and **16** (b). The most informative NOEs and  $^1\text{H}$ - $^1\text{H}$  coupling constants are given.

### Scheme 1



**21a** and recovery of the unchanged phosphine oxide **18** can be expected. In the case of an intermediate resulting

from the coupling of the isomeric phosphine oxide **17**, A-ring substituents do not exert an additional steric

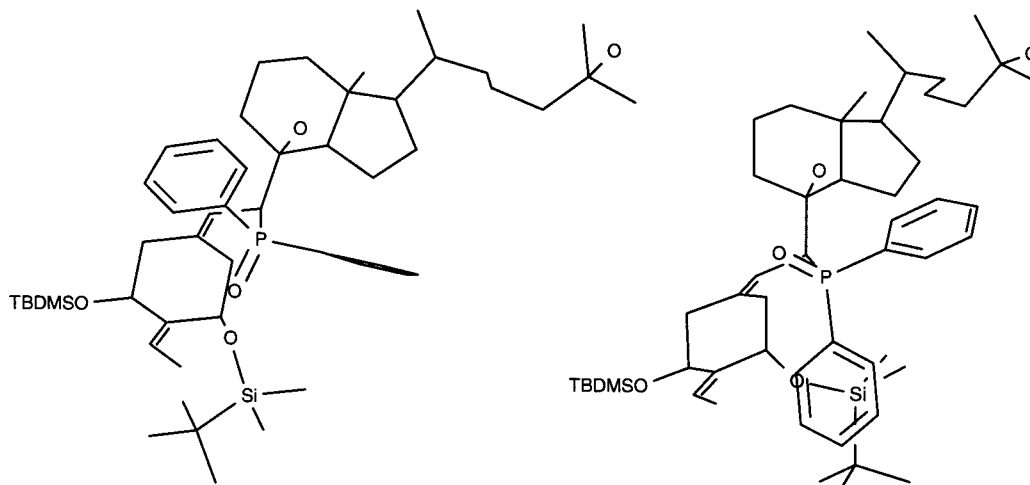
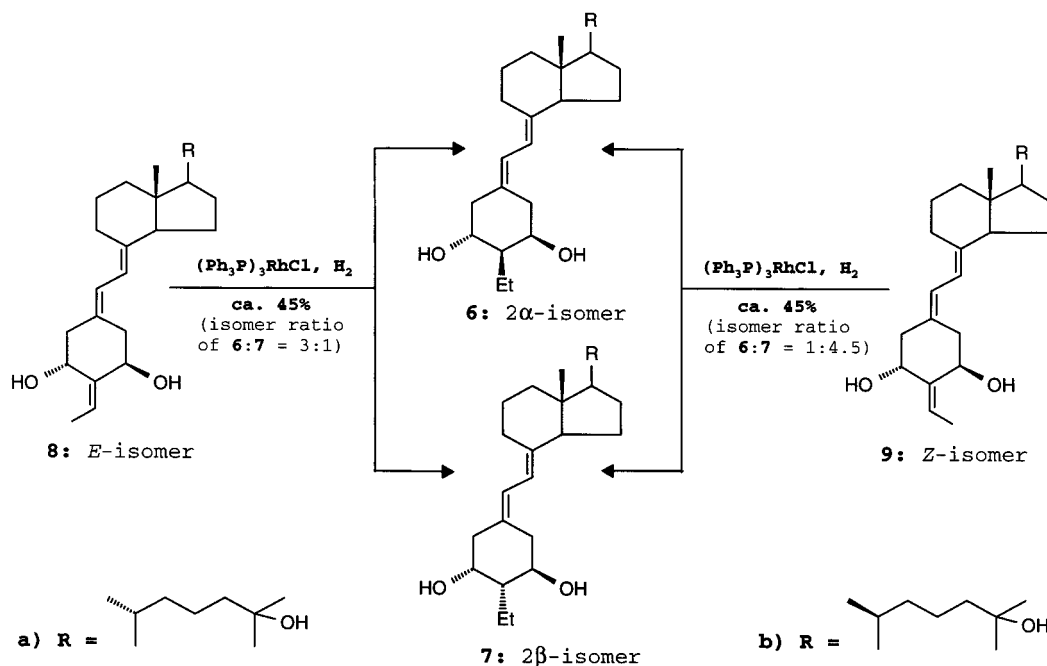


**Figure 3.** Stereoviews of the intermediates of the Wittig–Horner reaction between an anion of the phosphine oxide **18** and the ketone **19a**. Two conformers are shown with a torsional angle P–C(7)–C(8)–O set at 0°; all hydrogen atoms are omitted for clarity.

## Scheme 2



hindrance with phosphorus substituents and, as a consequence, do not prevent formation of the desired diene product **20a**.

Analogous to the procedure described above, Wittig–Horner coupling of **17** and **18** with the protected (20*S*)-25-hydroxy Grundmann's ketone **19b** provided 19-norvitamin D<sub>3</sub> compounds **20b** and **21b** in 90 and 15% yields, respectively. Deprotection of silyl protecting groups in the obtained condensation products **20a,b** and **21a,b** gave 2-ethylidene-19-norvitamins **8a,b** and **9a,b** (56–75% yield), respectively. They were, in turn, subjected to homogeneous catalytic hydrogenation with Wilkinson's catalyst (Scheme 2), and the corresponding pairs of 2 $\alpha$ - and 2 $\beta$ -ethyl-19-norvitamins **6a,7a** and **6b,7b**, formed in ca. 45% yield, were easily separated by HPLC. The stereochemistry at C-2 in the synthesized vitamin D compounds was tentatively determined on the basis of conformational analysis, molecular modeling, and <sup>1</sup>H NMR spectroscopy.

**Conformational Analysis.** It has been established that ring A of vitamin D<sub>3</sub>, 1 $\alpha$ -hydroxyvitamin D<sub>3</sub>, and the natural hormone **1**<sup>13</sup> and its analogues<sup>14</sup> exist in solution as two chair forms (named  $\alpha$  and  $\beta$ , Figure 4a) in rapid equilibrium.<sup>15</sup> Of particular interest are compounds in which, due to some modifications of their structures, such conformational equilibrium is strongly shifted to one particular A-ring chair form. Biological testing of such compounds could possibly provide some insight into an intriguing question as to which conformation of ring A in vitamin D compounds is responsible for its biological action. In an attempt to solve this problem, the 2-methyl analogues of the natural hormone<sup>16</sup> and 19-nor-1 $\alpha$ ,25-(OH)<sub>2</sub>D<sub>3</sub><sup>6</sup> were synthesized. Clearly, the presence of a bulky 2-alkyl substituent results in a significant bias toward one chair form of the A-ring (Figure 4b). Therefore, the 2-ethyl group, characterized by a large conformational free energy *A* value (1.75 kcal/mol)<sup>17</sup> similar to that of the methyl

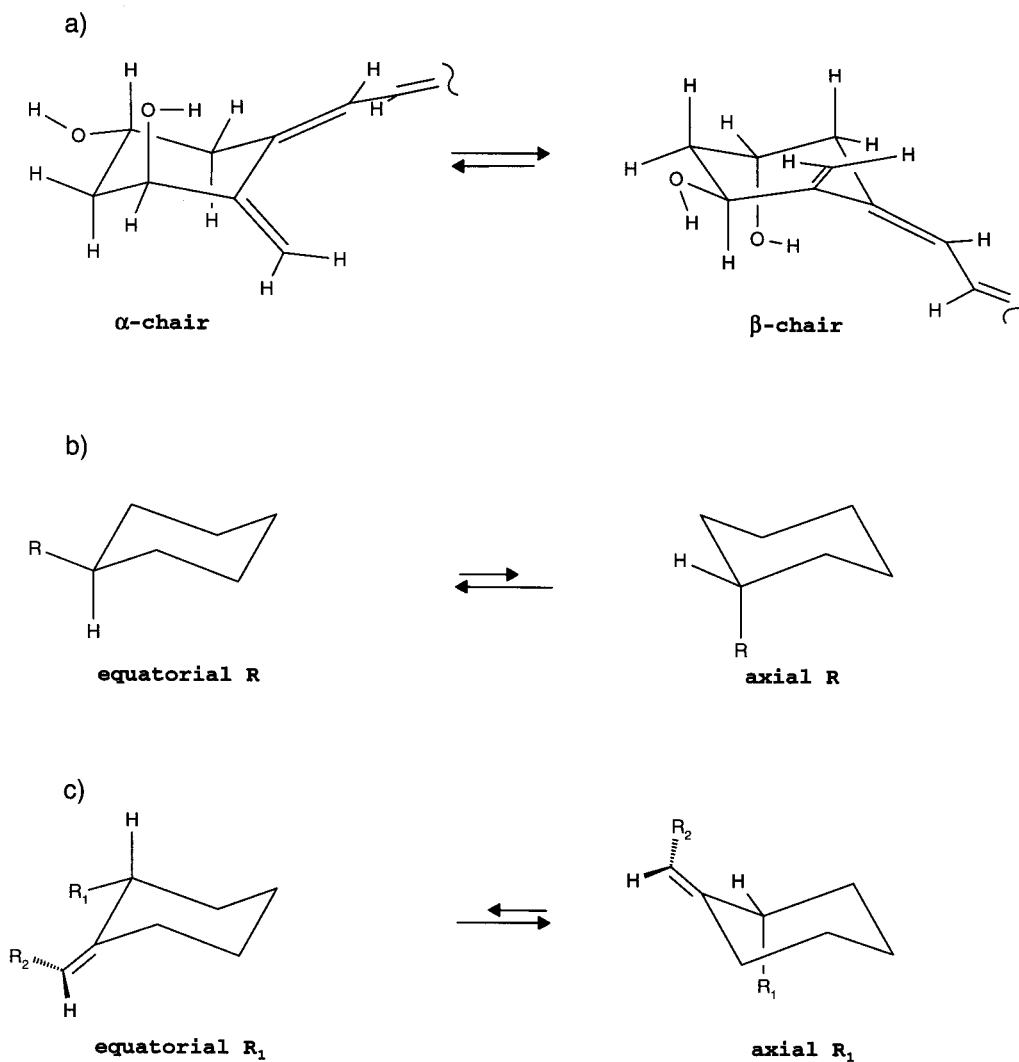


**Figure 4.** Conformational equilibrium in ring A of 1 $\alpha$ -hydroxyvitamin D<sub>3</sub> analogues (a), monosubstituted cyclohexanes (b), and 2-substituted alkylidenecyclohexanes (c).

group (1.70 kcal/mol),<sup>17</sup> should exert a similar effect on the A-ring conformation, shifting the equilibrium toward the conformers with the equatorial C-2-ethyl substituents. In the obtained 2-ethylidene-19-norvitamin D<sub>3</sub> compounds, a different strong interaction (designated as A<sup>(1,3)</sup>-strain,<sup>18,19</sup> Figure 4c) existing between the methyl group from the ethylidene moiety and equatorial hydroxyls at C-1 or C-3 should be involved. This should result in the strong bias toward conformers with an axial orientation of this hydroxy group to which the methyl from the ethylidene fragment is directed.

Molecular modeling fully supported these assumptions regarding the structure of vitamin D compounds described in the present work. The preferred A-ring conformations of isomeric 2-ethyl- and 2-ethylidene-substituted 19-norvitamins (Figure 5) were established by force field calculations (PC MODEL 6.0, Serena Software)<sup>20</sup> performed on model compounds lacking side chains. Also, analysis of the <sup>1</sup>H NMR spectra of the final vitamins leads to the same conclusions. Thus, for example, the magnitudes of vicinal coupling constants (13.7, 3.9 Hz) of the 10 $\alpha$ -H proton signal ( $\delta$  2.87) in the 2 $\alpha$ -ethyl vitamin **6a** support its equatorial disposition,<sup>21</sup> whereas the multiplet pattern of 4 $\beta$ -H at  $\delta$  2.14 (t,  $J \sim 11$  Hz) is typical of an axial hydrogen. However, in

vitamin **8a**, large coupling constants of the same 10 $\alpha$ -H, resonating at  $\delta$  1.85 (br t,  $J \sim 12$  Hz), indicated its trans-diaxial relationship with the vicinal 1 $\beta$ -H and, consequently, significant bias toward a chair conformation possessing 1 $\alpha$ - and 3 $\beta$ -hydroxyls in an equatorial and axial orientation, respectively.

As expected, <sup>1</sup>H NMR spectra of 2-ethyl vitamins **6a,b** and **7a,b** were very similar to those of the previously synthesized 2-methyl analogues **4a,b** and **5a,b**.

**Biological Evaluation.** The problem of the A-ring form required for biological activity of vitamin D has been discussed since 1974 when Okamura et al.<sup>22</sup> postulated that calcium regulation ability is limited to vitamin D compounds which can assume a conformation with the 1 $\alpha$ -hydroxy group (commonly considered as the substituent crucial for biological activity) occupying the equatorial position. According to this hypothesis, such geometry of the A-ring is required for binding to the vitamin D receptor and induction of subsequent biological responses involving transport and mobilization of the calcium in the body. The results of our biological studies on 1 $\alpha$ ,25-dihydroxy-10,19-dihydrovitamin D<sub>3</sub> analogues described in 1994<sup>23</sup> stood in some contrast with Okamura's suggestion because it was found that the 1 $\alpha$ -hydroxy group in the most calcemic 10*S*-isomer,

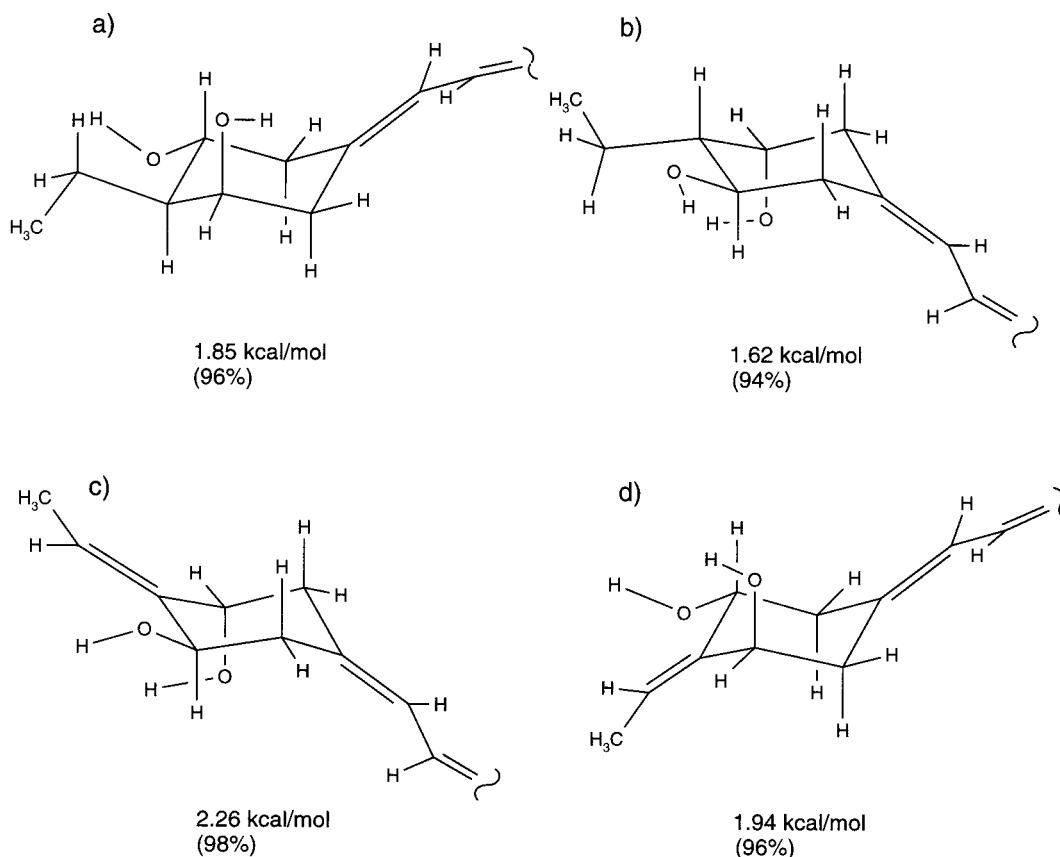


**Figure 5.** Preferred, energy-minimized (PC MODEL 6.0, Serena Software) A-ring conformations of the synthesized analogues **6a,b** (a), **7a,b** (b), **8a,b** (c), and **9a,b** (d). Steric energy differences between the preferred conformers and their partners with the inverted chair forms (calculated for model compounds lacking side chain) are given. Corresponding percentage populations (in parentheses) of conformers are given for room temperature (25 °C).

possessing the strongly preferred A-ring conformation, occupies an axial position. Recent structure–activity studies performed on 2-substituted analogues of natural hormone<sup>16</sup> and 19-nor-1 $\alpha$ ,25-(OH)<sub>2</sub>D<sub>3</sub><sup>6</sup> indicated a similar relationship between the orientation of 1 $\alpha$ -OH<sup>24</sup> and biological activity. Thus, in the preferred A-ring conformation of these vitamins, a bulky alkyl (hydroxy-alkyl) substituent occupies an equatorial orientation. Consequently, the 1 $\alpha$ -hydroxyl in 2 $\alpha$ - and 2 $\beta$ -substituted vitamins must be oriented axially and equatorially, respectively. Biological data strongly indicate that 2 $\alpha$ -alkyl vitamins have considerably higher calcemic activity than their 2 $\beta$ -substituted counterparts, and this trend is particularly remarkable in the 20*S*-series. An interesting input to the problem of importance of one particular A-ring conformation of vitamin D analogues came from the very recent studies of the crystal structure of the VDR. Although the VDR and its complex with hormone **1** resisted all attempts at crystallization, the Moras group succeeded in getting the crystals of **1** complexed with the hVDR mutant (118–425,  $\Delta$ [165–215]).<sup>25</sup> The reported X-ray crystallographic data of this receptor, complexed with **1** as well as with its analogues with the modified side chain,<sup>26</sup> revealed that in all cases these vitamins were present with their A-rings in  $\beta$ -chair form and with equatorially oriented 1 $\alpha$ -hydroxy groups. Moreover, the hydroxy groups in the examined analogues, including 20-epi compounds MC 1288 and KH 1060, bound the receptor making the same contacts within the binding pocket. The main difference between

the complexes with the natural ligand and its 20-epi analogues is the position of the methyl group at C-20 which is situated in the latter compounds closer to His 397. The fact that 20-epi compounds protect the VDR against degradation<sup>27</sup> more efficiently than the natural hormone **1** and the observation that double mutation (at positions 421 and 422)<sup>28</sup> in hVDR is important only for binding of 20-epi analogues but not for the hormone seem to suggest different conformations of VDR in the complexes mentioned above. These results are in contrast with the crystal structures of the hVDR deletion mutant complexes (118–425,  $\Delta$ [165–215]) with the hormone or 20-epi analogues<sup>26</sup> where the overall conformation of hVDRmt and the position of H12 are strictly maintained.

It should also be noted that one of the mutations of hVDR (S278A) was described<sup>29</sup> that did not affect the affinity for **1** and, therefore, did not confirm a contact between Ser 278 and the ligand's hydroxyl at C-3. This may suggest that the *in vivo* conformation of the liganded **1** can be different from that reported for its crystals with hVDRmt. When the facts described above are considered, it could be concluded that the role of 1 $\alpha$ -hydroxyl orientation and A-ring conformation in the biological profile of the vitamin D molecule is still unclear, and additional information is needed.

The synthesized vitamins **6a,b**–**9a,b** were tested for their ability to bind the porcine intestinal vitamin D receptor. The presented results (Table 1) indicate that 2 $\alpha$ -ethyl-19-norvitamins **6a** and **6b** bind the receptor

**Table 1.** VDR Binding Properties<sup>a</sup> and HL-60 Differentiating Activities<sup>b</sup> of 2-Substituted Analogues of 1 $\alpha$ ,25-Dihydroxy-19-norvitamin D<sub>3</sub> and Their 20*S*-Isomers

compound	compd no.	VDR binding		HL-60 differentiation	
		ED <sub>50</sub> (M)	binding ratio	ED <sub>50</sub> (M)	activity ratio
1 $\alpha$ ,25-(OH) <sub>2</sub> D <sub>3</sub>	<b>1</b>	5.0 × 10 <sup>-10</sup>	1	2.7 × 10 <sup>-9</sup>	1
2 $\alpha$ -ethyl-19-nor-1 $\alpha$ ,25-(OH) <sub>2</sub> D <sub>3</sub>	<b>6a</b>	6.0 × 10 <sup>-10</sup>	1.2	4.6 × 10 <sup>-10</sup>	0.17
2 $\beta$ -ethyl-19-nor-1 $\alpha$ ,25-(OH) <sub>2</sub> D <sub>3</sub>	<b>7a</b>	5.0 × 10 <sup>-8</sup>	100	1.2 × 10 <sup>-8</sup>	4.4
2 $\alpha$ -ethyl-19-nor-(20 <i>S</i> )-1 $\alpha$ ,25-(OH) <sub>2</sub> D <sub>3</sub>	<b>6b</b>	2.5 × 10 <sup>-10</sup>	0.5	1.3 × 10 <sup>-10</sup>	0.05
2 $\beta$ -ethyl-19-nor-(20 <i>S</i> )-1 $\alpha$ ,25-(OH) <sub>2</sub> D <sub>3</sub>	<b>7b</b>	3.0 × 10 <sup>-9</sup>	6.0	6.3 × 10 <sup>-9</sup>	2.3
1 $\alpha$ ,25-(OH) <sub>2</sub> D <sub>3</sub>	<b>1</b>	6.0 × 10 <sup>-10</sup>	1	2.5 × 10 <sup>-9</sup>	1
2-ethylidene-19-nor-1 $\alpha$ ,25-(OH) <sub>2</sub> D <sub>3</sub> ( <i>E</i> -isomer)	<b>8a</b>	2.5 × 10 <sup>-10</sup>	0.4	2.0 × 10 <sup>-9</sup>	0.8
2-ethylidene-19-nor-1 $\alpha$ ,25-(OH) <sub>2</sub> D <sub>3</sub> ( <i>Z</i> -isomer)	<b>9a</b>	7.0 × 10 <sup>-9</sup>	12	4.0 × 10 <sup>-9</sup>	1.6
2-ethylidene-19-nor-(20 <i>S</i> )-1 $\alpha$ ,25-(OH) <sub>2</sub> D <sub>3</sub> ( <i>E</i> -isomer)	<b>8b</b>	2.8 × 10 <sup>-10</sup>	0.5	2.2 × 10 <sup>-10</sup>	0.09
2-ethylidene-19-nor-(20 <i>S</i> )-1 $\alpha$ ,25-(OH) <sub>2</sub> D <sub>3</sub> ( <i>Z</i> -isomer)	<b>9b</b>	5.0 × 10 <sup>-10</sup>	0.8	1.5 × 10 <sup>-10</sup>	0.06

<sup>a</sup> Competitive binding of 1 $\alpha$ ,25-(OH)<sub>2</sub>D<sub>3</sub> (**1**) and the synthesized vitamin D analogues to the porcine intestinal vitamin D receptor. The experiments were carried out in triplicate on two different occasions. The ED<sub>50</sub> values are derived from dose–response curves and represent the analogue concentration required for 50% displacement of the radiolabeled 1 $\alpha$ ,25-(OH)<sub>2</sub>D<sub>3</sub> from the receptor protein. The binding ratio is the ratio of the analogue average ED<sub>50</sub> to the ED<sub>50</sub> for 1 $\alpha$ ,25-(OH)<sub>2</sub>D<sub>3</sub>. <sup>b</sup> Induction of differentiation of HL-60 promyelocytes to monocytes by 1 $\alpha$ ,25-(OH)<sub>2</sub>D<sub>3</sub> (**1**) and the synthesized vitamin D analogues. The differentiation state was determined by measuring the percentage of cells reducing nitro blue tetrazolium (NBT). The experiment was repeated three times. The ED<sub>50</sub> values are derived from dose–response curves and represent the analogue concentration capable of inducing 50% maturation. The differentiation activity ratio is the ratio of the analogue average ED<sub>50</sub> to the ED<sub>50</sub> for 1 $\alpha$ ,25-(OH)<sub>2</sub>D<sub>3</sub>.

better than their isomers with the 2 $\beta$ -ethyl substituent. In the series of 2-ethyl analogues, 20-epimerization increases the binding potency, especially (17 times) for the 2 $\beta$ -isomers (**7a** versus **7b**). Similar trends were observed previously for 2-methyl-substituted 19-norvitamins<sup>6</sup> and derivatives of the natural hormone.<sup>16d,e</sup> The competitive binding analysis showed that 2-ethylidene-19-norvitamins possessing the methyl group from the ethylidene moiety directed toward C-3, that is, trans in relation to the C(6)–C(7) bond (*E*-isomers), are more active than 1 $\alpha$ ,25-(OH)<sub>2</sub>D<sub>3</sub> in binding to VDR; their counterparts with the cis relationship between the ethylidene methyl substituent and C(7)–H group (*Z*-isomers) exhibit reduced affinity for the receptor. It is interesting that 20-epimerization does not influence the binding ability of the *E*-isomer (**8a** versus **8b**), while it significantly increases (15 times) the potency of the *Z*-isomer form (**9a** versus **9b**). Our previous work indicated that the binding potency of 2-methylene-substituted 19-norvitamins is not affected by 20-epimerization.<sup>6</sup>

In the next assay, the cellular activity of the synthesized compounds was established by studying their ability to induce differentiation of human promyelocyte HL-60 cells into monocytes. Both 2 $\alpha$ -ethyl-19-norvitamins and both isomers (*E* and *Z*) of (20*S*)-2-ethylidene-19-norvitamin D<sub>3</sub> are more potent than 1 $\alpha$ ,25-(OH)<sub>2</sub>D<sub>3</sub> in this assay (Table 1), whereas the remaining tested compounds are almost equivalent to hormone **1**. Both *E*-isomers of the 2-ethylidene-19-norvitamins, when tested in vivo in rats (Table 2), exhibited high calcemic activity with the 20*S*-compound being especially potent. The isomeric *Z* compounds are significantly less potent, having no intestinal calcium transport activity. 2-Ethyl-19-norvitamins have some ability to mobilize calcium from bone but not to the extent of hormone **1**; however, they are inactive in the intestine. The only exception is the 2 $\alpha$ -ethyl isomer from the 20*S*-series which exhibits a strong calcium mobilization response and marked intestinal activity. Comparison of biological in vitro and in vivo activities of 2-ethyl- and 2-ethylidene-19-norvitamins exhibits, rather to our surprise, that their potency seems to not be influenced by the orientation

of the 1 $\alpha$ -hydroxy group in their preferred A-ring conformations.

**Receptor Modeling and Ligand Docking. 1. Model of the Full-Length Ligand Binding Domain of Rat VDR.** The vitamin D receptor (VDR) shares its “ $\alpha$ -helical sandwich structure” with other members of the nuclear receptor (NR) superfamily which includes receptors for the steroid, retinoid, and thyroid hormones.<sup>29–31</sup> Interestingly, ligands which bind to the respective proteins (ER, PR, RAR, and VDR) are harbored in the same region in all members of the NR family.<sup>29</sup> The VDR is most closely related in architecture to the RAR. Such structural similarity, delineated from homology modeling, was verified by the crystal structure of the hVDR (118–425,  $\Delta$ [165–215]) mutant.<sup>25</sup>

Although the architecture of the vitamin D receptor resembles those of other nuclear receptors, it contains one distinct feature: a long insertion domain connecting helices H1 and H3. This highly nonhomologous fragment covers 72–81 residues in the VDR family compared to 15–25 residues in other members of the NR family. The domain, encompassing residues 165–215 in hVDR, is poorly conserved in different VDR species (9% identity between amino acids 157 and 215). Until now, only one biological function (phosphorylation) has been found for this unique fragment.<sup>32</sup> Its presence hampers the efforts directed toward establishing the VDR structure because this fragment is probably responsible for the decreased crystallization ability of the protein and, at the same time, creates serious problems in protein homology modeling. Therefore, it is not surprising that even in a recently calculated hVDR molecular model,<sup>33</sup> fragment 162–221 was excised because of the absence of any structural information on which homology modeling could be based. However, we have reported that by employing lattice modeling (SICHO (SIDE-CHAIN ONLY) method) for a folding of poorly structured parts (residues 120–164) of the rat VDR, a structure highly consistent with the crystal structure of the hVDR mutant was retrieved.<sup>34</sup>

In this paper, the first model of the full-length ligand binding domain of rVDR (118–423) was constructed. The same method, which combined homology and lattice

**Table 2.** Support of Intestinal Calcium Transport and Bone Calcium Mobilization by 2-Substituted Analogues of 1 $\alpha$ ,25-Dihydroxy-19-norvitamin D<sub>3</sub> in Vitamin D-Deficient Rats on a Low-Calcium Diet<sup>a</sup>

compound	compd no.	amount (pmol)	Ca transport S/M (mean $\pm$ SEM)	serum Ca (mean $\pm$ SEM)
none (control)		0	3.8 $\pm$ 0.4 <sup>b</sup>	3.9 $\pm$ 0.1 <sup>b</sup>
1 $\alpha$ ,25-(OH) <sub>2</sub> D <sub>3</sub>	<b>1</b>	260	6.5 $\pm$ 0.9 <sup>c</sup>	5.8 $\pm$ 0.1 <sup>c</sup>
2 $\alpha$ -ethyl-19-nor-1 $\alpha$ ,25-(OH) <sub>2</sub> D <sub>3</sub>	<b>6a</b>	260	4.0 $\pm$ 0.4 <sup>d</sup>	5.1 $\pm$ 0.1 <sup>d</sup>
2 $\beta$ -ethyl-19-nor-1 $\alpha$ ,25-(OH) <sub>2</sub> D <sub>3</sub>	<b>7a</b>	260	3.7 $\pm$ 0.3 <sup>e</sup>	5.0 $\pm$ 0.1 <sup>e</sup>
2 $\alpha$ -ethyl-19-nor-(20S)-1 $\alpha$ ,25-(OH) <sub>2</sub> D <sub>3</sub>	<b>6b</b>	260	5.0 $\pm$ 0.4 <sup>f</sup>	7.0 $\pm$ 0.1 <sup>f</sup>
2 $\beta$ -ethyl-19-nor-(20S)-1 $\alpha$ ,25-(OH) <sub>2</sub> D <sub>3</sub>	<b>7b</b>	260	4.1 $\pm$ 0.3 <sup>g</sup>	5.6 $\pm$ 0.1 <sup>g</sup>
none (control)		0	3.0 $\pm$ 0.7 <sup>b</sup>	4.3 $\pm$ 0.1 <sup>b</sup>
1 $\alpha$ ,25-(OH) <sub>2</sub> D <sub>3</sub>	<b>1</b>	130	5.5 $\pm$ 0.5 <sup>c1</sup>	5.1 $\pm$ 0.3 <sup>c1</sup>
		260	5.9 $\pm$ 0.4 <sup>c2</sup>	5.8 $\pm$ 0.3 <sup>c2</sup>
2-ethylidene-19-nor-1 $\alpha$ ,25-(OH) <sub>2</sub> D <sub>3</sub> ( <i>E</i> -isomer)	<b>8a</b>	65	5.0 $\pm$ 0.4 <sup>d1</sup>	4.5 $\pm$ 0.1 <sup>d1</sup>
		130	6.8 $\pm$ 0.4 <sup>d2</sup>	5.2 $\pm$ 0.2 <sup>d2</sup>
2-ethylidene-19-nor-1 $\alpha$ ,25-(OH) <sub>2</sub> D <sub>3</sub> ( <i>Z</i> -isomer)	<b>9a</b>	65	4.4 $\pm$ 0.4 <sup>e1</sup>	4.4 $\pm$ 0.2 <sup>e1</sup>
		130	5.7 $\pm$ 0.9 <sup>e2</sup>	4.2 $\pm$ 0.0 <sup>e2</sup>
none (control)		0	4.4 $\pm$ 0.2 <sup>b</sup>	4.1 $\pm$ 0.2 <sup>b</sup>
1 $\alpha$ ,25-(OH) <sub>2</sub> D <sub>3</sub>	<b>1</b>	130	4.9 $\pm$ 0.7 <sup>c1</sup>	5.2 $\pm$ 0.2 <sup>c1</sup>
		260	6.0 $\pm$ 0.9 <sup>c2</sup>	6.4 $\pm$ 0.4 <sup>c2</sup>
2-ethylidene-19-nor-(20S)-1 $\alpha$ ,25-(OH) <sub>2</sub> D <sub>3</sub> ( <i>E</i> -isomer)	<b>8b</b>	65	9.0 $\pm$ 0.3 <sup>d1</sup>	8.2 $\pm$ 0.3 <sup>d1</sup>
		130	5.8 $\pm$ 0.8 <sup>d2</sup>	12.1 $\pm$ 0.6 <sup>d2</sup>
none (control)		0	4.6 $\pm$ 0.4 <sup>b</sup>	4.3 $\pm$ 0.1 <sup>b</sup>
1 $\alpha$ ,25-(OH) <sub>2</sub> D <sub>3</sub>	<b>1</b>	65	5.2 $\pm$ 0.6 <sup>c1</sup>	5.7 $\pm$ 0.1 <sup>c1</sup>
		130	6.0 $\pm$ 0.7 <sup>c2</sup>	6.4 $\pm$ 0.1 <sup>c2</sup>
2-ethylidene-19-nor-1 $\alpha$ ,25-(OH) <sub>2</sub> D <sub>3</sub> ( <i>Z</i> -isomer)	<b>9b</b>	65	6.6 $\pm$ 0.8 <sup>d1</sup>	4.4 $\pm$ 0.1 <sup>d1</sup>
		130	6.7 $\pm$ 0.2 <sup>d2</sup>	5.1 $\pm$ 0.3 <sup>d2</sup>

<sup>a</sup> Weanling male rats were maintained on a 0.47% Ca diet for 1 week, and then switched to a low-calcium diet containing 0.02% Ca for an additional 3 weeks. Over the last week, they were dosed daily with the appropriate vitamin D compound for 7 consecutive days. All doses were administered intraperitoneally in 0.1 mL of propylene glycol/ethanol (95:5). Controls received the vehicle. Determinations were made 24 h after the last dose. There were at least 6 rats per group. Statistical analysis was done by Student's *t* test. Statistical data: serosal/mucosal (S/M), panel 1, b from c, *p* < 0.01, b from d, e, and g, NS, b from f, *p* = 0.01; panel 2, b from c<sup>1</sup>, d<sup>1</sup>, and e<sup>1</sup>, NS, b from c<sup>2</sup>, *p* = 0.001, b from d<sup>2</sup>, *p* < 0.001, b from e<sup>2</sup>, *p* < 0.025; panel 3, b from c<sup>1</sup> and d<sup>2</sup>, NS, b from c<sup>2</sup>, *p* = 0.025, b from d<sup>1</sup>, *p* < 0.001; panel 4, b from c<sup>1</sup>, NS, b from c<sup>2</sup>, d<sup>1</sup>, and d<sup>2</sup>, *p* < 0.005; serum calcium, panel 1, b from c, f, and g, *p* < 0.001, b from d and e, *p* < 0.005; panel 2, b from c<sup>1</sup> and d<sup>2</sup>, *p* < 0.025, b from d<sup>1</sup>, e<sup>1</sup>, and e<sup>2</sup>, NS, b from c<sup>2</sup>, *p* < 0.001; panel 3, b from c<sup>1</sup>, *p* < 0.005, b from c<sup>2</sup>, d<sup>1</sup>, and d<sup>2</sup>, *p* < 0.001; panel 4, b from c<sup>1</sup> and c<sup>2</sup>, *p* = 0.001, b from d<sup>1</sup> and d<sup>2</sup>, NS.

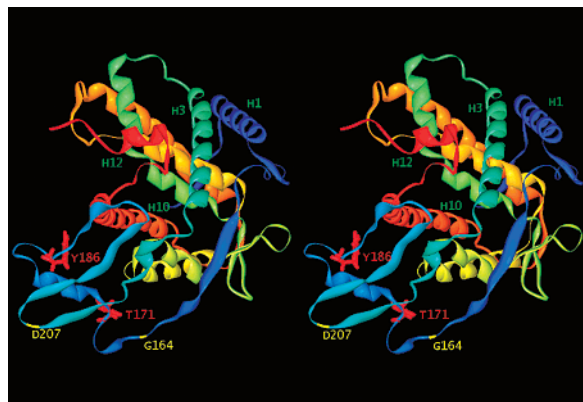


**Figure 6.** Stereoview of the three-dimensional structure of rat VDR. The nonhomologous part of the receptor between long helices H1 and H3 (residues 164–207, colored in blue) was modeled by SICHO.

modeling and was used successfully for creating two simplified rVDR models,<sup>34</sup> was also employed in this work. The nonhomologous portion of the VDR receptor, excised in crystallized hVDRmt, was modeled by the program SICHO<sup>35</sup> and is shown in Figure 6. It is readily observed that the lattice-modeled domain (residues 164–207) is highly disordered and does not contain any well-structured elements. This unique VDR part of the protein forms loops, spanning between amino acids Ser 178–Asn 204 and Ser 205–Ser 218. The poorly structured architecture of the domain, delineated from lattice modeling, remains in excellent agreement with structural investigations (SAXS) performed in solution.<sup>36</sup> It

is also known that removal of the domain 165–215 has no major effect on ligand binding, transactivation, or dimerization of the vitamin D receptor with RXR.<sup>25</sup> Our model shows that the region connecting helices H1 and H3 is distant from the pocket and, therefore, is unlikely to affect the binding abilities of the ligand. This structure is confirmed by an experiment indicating that mutation C190W (hVDR) does not influence the binding function of the receptor.<sup>37a</sup> Moreover, according to our computational model, the disordered domain (164–207) is sufficiently remote from the receptor region involved in transcription (H12) and dimerization with RXR (H3). Further evidence supporting our model comes from the observation that hVDR is sensitive to proteolysis with a trypsin cleavage site after Arg 174.<sup>37b</sup> The region in rVDR, compatible with the above-mentioned domain, begins with Thr 171 which is situated on the remote edge of the protein (Figure 6).

Superimposition of the full-length rat VDR-LBD model and RAR crystal structure is shown in Figure 7. With the exclusion of the highly disordered VDR loop (164–207), the proteins overlaid with an RMSD of 2.52 Å over 156 residues (compared by using the Gerstein and Levitt structural alignment algorithm).<sup>38</sup> It is worth mentioning that experimental data supporting our full model of rVDR come from different kinds of experiments, covering structural investigation in solution as well as biological activities.

**2. Docking Experiments.** Until the present time, only complexes of the hVDR deletion mutant (118–425,  $\Delta$  [165–215]) with vitamin D analogues possessing an

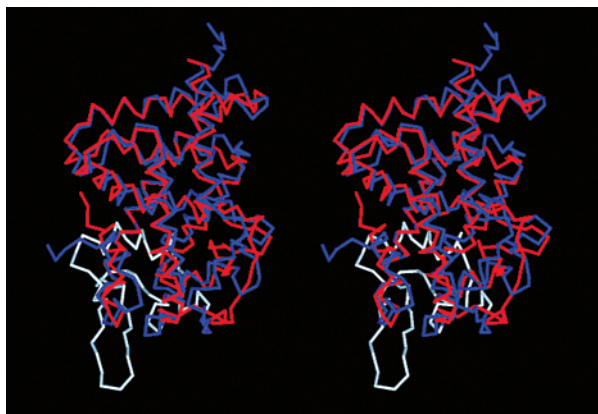


**Figure 7.** Stereoview of the superimposition of the rat VDR-LBD model (blue) and human RAR (red). Part of rVDR modeled by SICHO (residues 164–207) is colored in light blue.

unmodified A-ring (i.e., analogous to that of the hormone) have been crystallized. It was found that side chain-modified analogues with a natural configuration at C-20 (MC 903, EB 1089, and TX 522) bind to the hVDRmt in a fashion similar to that of  $1\alpha,25\text{-(OH)}_2\text{D}_3$ .<sup>26a</sup> Thus, the A-ring is always oriented toward Tyr 143, and the side chain hydroxyl at C-25 contacts the same amino acids (His 305 and His 397). Also, the  $1\alpha\text{-OH}$  group in the analogues creates hydrogen bonds with Ser 237 and Arg 274, while  $3\beta\text{-OH}$  creates bonds with Ser 278 and Tyr 143.<sup>25</sup>

In the present work, we performed docking simulations of the four synthesized vitamins **6a–9a** possessing the same side chain as the natural hormone **1**. When the significant differences in their binding affinity for VDR were taken into account, it was interesting to establish how they could accommodate the binding pocket. These four vitamins were docked into full-length rVDR-LBD in their energy-minimized conformations (see Experimental Section). The docking procedure employed in this work was verified by modeling complexes between full-length rVDR-LBD and natural hormone **1** that was introduced into the binding pocket by an A-ring or side chain. Regardless of such different positioning,  $1\alpha,25\text{-(OH)}_2\text{D}_3$  was finally oriented in the pocket in the “native” fashion. Our docking experiments performed with 19-norvitamins **6a–9a** revealed that the binding pocket consists of eleven amino acids common for all modeled complexes: His 225, Leu 226, Val 230, Ile 264, Glu 265, Met 268, Trp 282, Cys 284, Lys 290, Tyr 291, and His 393 (Figure 8, residues marked in green). It is worth mentioning that His 393 also forms hydrogen bonds to 25-OH in the “native” complex. Involvement of the amino acids His 225, Val 230, Trp 282, Cys 284, and His 393 in hormone binding was verified by mutations<sup>34</sup> as well as affinity labeling<sup>39</sup> and is in agreement with contacts found in the rVDR pocket that accommodated 19-nor analogues. The existence of contacts between glutamic acid (Glu 265) and A-ring-functionalized analogues is supported by newly published data.<sup>27</sup> The studies on point mutation E269A of hVDR allowed the authors to suggest that Glu 269 may have a role in stabilizing the conformation of the receptor after ligand binding. The presence of Trp 282 and Cys 284 in the VDR binding pocket was confirmed by several methods.<sup>25,40</sup> It is worth noting that in all

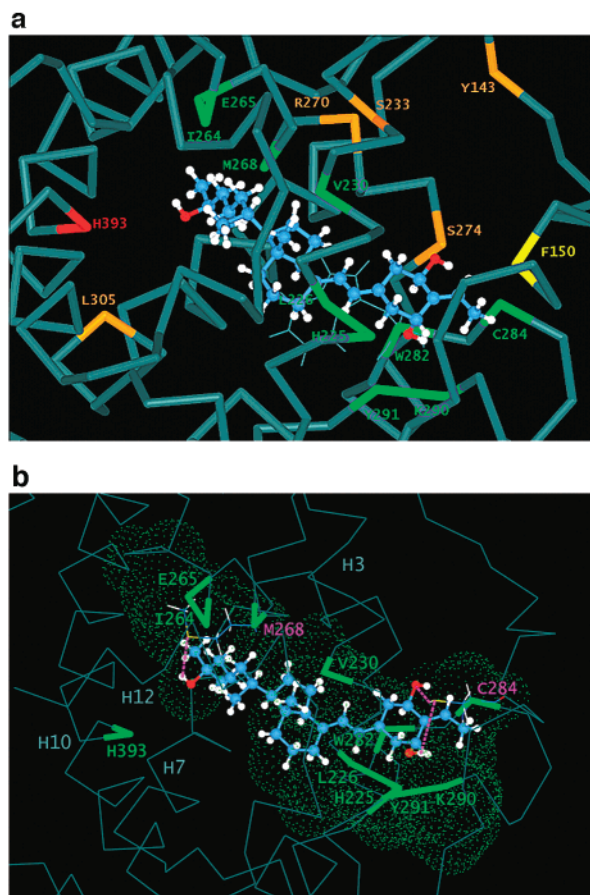


**Figure 8.** View of the three-dimensional structure of the ligand binding cavity of the modeled rat VDR with the docked vitamin D analogue **8a**. The common contacts (distances shorter than 3.5 Å) found between any atom of the ligands (**6a–9a**) and receptor are marked in green. (a) Residues of the human VDRmt (118–425,  $\Delta$ [165–215]), creating contacts with the hydroxy groups of the hormone, are marked in orange. His 393, being in contact sites for the hormone and the 19-norvitamins **6a–9a**, is marked in red. Ring A of the hormone is directed toward Tyr 143 and Phe 150. Tryptophan is situated close to the intericyclic diene fragment of the hormone and 19-norvitamins, and its indole ring is directed toward the A-ring of the ligands. (b) The most important hydrogen bonds with ligand's hydroxyls and Cys 284 and Met 268 are marked in magenta. Spatial regions within 3.5 Å of the contact residues lining the pocket are shown as spheres (green dots).

modeled complexes of analogues **6a–9a** with the full-length rVDR-LBD, tryptophan is located under the vitamin 5,7-diene fragment (similarly as in the crystalline “native” complex)<sup>25</sup> and directs its indole-ring toward the A-ring of the vitamin D compound (Figure 8a). Interestingly, the same set of amino acids creates hydrogen bonds with the hydroxyls of 2-ethyl and 2-ethylidene analogues. It was found that Met 268 and Tyr 291 contact 25- and  $3\beta$ -hydroxy groups, respectively. Cys 284 plays an important role in the binding of 2-ethylidene-19-norvitamins. In both complexes of analogues **8a** and **9a**, this amino acid bridges their A-ring hydroxyls; the formation of hydrogen bonds to  $1\alpha$ - and  $3\beta$ -OH groups can be especially effective in the case of the former *E*-isomer (Figure 8b) which, interestingly, shows the best ability to bind the porcine intestinal VDR. Also in the complex of 2 $\beta$ -ethyl compound **7a**, Cys

284 contacts its 1 $\alpha$ -OH substituent. In the case of the isomeric 2 $\alpha$ -ethyl analogue **6a**, its hydroxyl at C-1 is hydrogen-bonded to His 225 and Tyr 291. All 2-ethyl- and 2-ethylidene-19-norvitamins dock into the VDR binding pocket with their side chains in the lowest-energy (extended) conformation that stays in contrast with a side chain orientation detected for the hormone **1** in its crystalline complex.<sup>25</sup>

It was established that differences in the energies of the studied VDR complexes of 19-norvitamins **6a–9a** do not exceed 30 kcal/mol. Interestingly, analogues **7a** and **8a**, characterized by the greatest difference in binding affinity (100 times lower and 2.5 times higher than **1**, respectively), create complexes with significantly different energies of  $-85$  and  $-102$  kcal/mol (Figure 8), respectively, corresponding to the binding ability of the compounds. It seems that the highest binding potency of compound **8a** results not only from the strong contacts between its three hydroxyls and the receptor but also from stabilization of the ethylidene fragment by the amino acids Y 147, F 150, H 225, C 284, Y 289, and Y 291 which form channels surrounding this substituent. An aromatic ring of Phe 150 that is positioned parallel (3 Å) to the double bond of the ethylidene group can effectively stabilize it via  $\pi$ - $\pi$  interactions. Of the two 2-ethyl-19-norvitamin D<sub>3</sub> analogues **6a** and **7a**, the former compound with the alkyl group at C-2 in the  $\alpha$ -orientation ("up") binds VDR more effectively (83 times) than the latter ("down") 2 $\beta$ -isomer. A similar trend was observed for the C-2-alkylated hormone and its 5*E*-analogues.<sup>16d,e,41</sup> Inspection of our ligand-rVDR models of **6a** and **7a** indicates that the receptor creates weaker contacts to three hydroxy groups of the former compound. It seems that hydrophobic Leu 229, which is present in the vicinity of the 2 $\alpha$ -ethyl group in the complex of **6a**, stabilizes this substituent very effectively, and it could be responsible for the improvement of the binding ability of the analogue. We established previously<sup>6</sup> that introduction of the 2 $\alpha$ -methyl group into the 1 $\alpha$ ,25-dihydroxy-19-norvitamin D<sub>3</sub> molecule slightly (1.4 times) decreases its binding potency to VDR. In contrast, introduction of the 2 $\alpha$ -ethyl substituent results in increased VDR binding affinity (2.8 times) of the analogue. Interestingly, a completely opposite trend was observed for the C-2-functionalized hormone, where 2 $\alpha$ -methyl substitution increased (4 times) the binding potency while insertion of 2 $\alpha$ -ethyl decreased (2.5 times) it.<sup>41</sup> This might indicate that contacts in the binding pocket of A-ring-substituted analogues of the vitamin hormone differ from those of their 19-nor counterparts. Such a conclusion, deduced from binding activity studies, is in agreement with our docking computer experiment.

## Conclusions

The presented results confirm our earlier observations indicating that the introduction of different C-2-substituents into the parent 19-nor-1 $\alpha$ ,25-dihydroxyvitamin D<sub>3</sub> molecule can drastically change the biological activity of the analogues. Comparison of the biological potency of the synthesized 2 $\alpha$ -ethyl analogues with the previously reported data<sup>6</sup> for the corresponding 2 $\alpha$ -methyl-19-norvitamins clearly indicates that the increased size of the hydrophobic alkyl group at C-2 has an adverse

effect on biological potency. Also, the comparison of biological activities of the most active analogues in the 2-alkyl and 2-ethylidene series studied by us so far, that is, possessing 2 $\alpha$ -methyl (ethyl) and (*E*)-2-ethylidene substituents, indicates that their potency is not determined only by the axial and equatorial orientation, respectively, of the 1 $\alpha$ -hydroxy group in their preferred A-ring conformations. It is likely that differences in the accommodation of 2-alkyl (alkylidene) groups in the VDR pocket and their interactions with the surrounding amino acids can play a more important role. Biological data of 2-methylene-<sup>6</sup> and 2-ethylidene-19-norvitamin D<sub>3</sub> analogues show that such homologation of the alkylidene group at C-2 in the compound from the 20*S*-series provides the analogue (*E*-isomer) that has strong activity on bone and, additionally, is very effective on intestinal calcium transport.

Generally, compounds with an "unnatural" configuration at C-20 are characterized by significantly increased potency; explanation of this phenomenon would require additional studies. Over the last two years, several articles appeared highlighting an influence of 20-epimerization on biological activities of vitamin D compounds.<sup>26a,27,42,43</sup> It was found that a greater transcriptional potency (100 times) of 20-epi-1 $\alpha$ ,25-(OH)<sub>2</sub>D<sub>3</sub> is attributed primarily to its ability to enhance dimerization of VDR.<sup>42</sup> Recent studies also demonstrate the differences in target tissue metabolic paths of 1 $\alpha$ ,25-dihydroxy-20-epi vitamin D<sub>3</sub> and suggested that they are responsible for the increased biological activities of 20-epi vitamin D<sub>3</sub> analogues.<sup>43</sup>

The consistency of our full-length rVDR-LBD computational model with the experimentally outlined structure proves that lattice modeling of poorly homologous domains results in a model resembling the structure of the native protein. Automatic docking simulations performed by Flexi Dock software correctly positioned ligands in the VDR pocket, even when they were initially inversely situated in the protein cavity. Various analogues with different orientations of the 1 $\alpha$ -OH group (axial or equatorial) docked in the 6-(s)-trans conformation bind VDR in a similar way, being situated in the binding pocket with their A-ring oriented toward the interior of the cavity. 19-Norvitamin D<sub>3</sub> compounds modified with nonpolar C-2-substituents could be easily positioned in the receptor binding pocket because the amino acids lining the rVDR domain, the closest to C-2, are mostly hydrophobic. Although the differences in energy between complexes are small, they correspond to the binding potency of the analogues.

## Experimental Section

**Chemistry.** Optical rotations were measured in chloroform using a Perkin-Elmer 241 automatic polarimeter at 22 °C. Ultraviolet (UV) absorption spectra were recorded with a Hitachi model 60-100 UV-vis spectrometer in the solvent noted. <sup>1</sup>H and <sup>13</sup>C nuclear magnetic resonance (NMR) spectra were recorded at 500 and 125 MHz with a Bruker AM-500 FT spectrometer in deuteriochloroform. Chemical shifts ( $\delta$ ) are reported downfield from internal Me<sub>4</sub>Si ( $\delta$  0.00). Low- and high-resolution mass spectra were recorded at 70 eV on a Kratos DS-50 TC instrument equipped with a Kratos DS-55 data system. Samples were introduced into the ion source maintained at 120–250 °C via a direct insertion probe. High-performance liquid chromatography (HPLC) was performed on a Waters Associates liquid chromatograph equipped with

a model 6000A solvent delivery system, a model 6 UK Universal injector, a model 486 tunable absorbance detector, and a differential R 401 refractometer. Microanalysis of crystalline compounds was within  $\pm 0.4\%$  of the theoretical values. THF was freshly distilled from sodium benzophenone ketyl under argon before use.

The starting hydroxy ketone **10** was obtained from commercial (–)-quinic acid as described previously.<sup>10</sup> **10**: mp 98–100 °C (from hexane);  $[\alpha]_D^{25} -19.2^\circ$  (*c* 0.9, CHCl<sub>3</sub>); <sup>1</sup>H NMR (CDCl<sub>3</sub>)  $\delta$  0.067, 0.086, and 0.092 (6H, 3H, and 3H, each s, 4  $\times$  SiCH<sub>3</sub>), 0.856 and 0.899 (9H and 9H, each s, 2  $\times$  Si-*t*-Bu), 2.25 (1H, ddd, *J* = 14.4, 4.0, 1.8 Hz), 2.45 (1H, ddd, *J* = 14.0, 5.2, 1.0 Hz), 2.60 (1H, dd, *J* = 14.0, 10.2 Hz), 2.77 (1H, ddd, *J* = 14.4, 3.5, 1.0 Hz), 3.80 (1H, ~d, *J* = 4 Hz), 4.27 (2H, m); <sup>13</sup>C NMR (CDCl<sub>3</sub>)  $\delta$  –5.08 (q), –4.93 (q), –4.88 (q), –4.74 (q), 17.86 (s), 18.02 (s), 25.59 (q), 25.74 (q), 44.28 (t), 45.98 (t), 69.41 (d), 70.04 (d), 72.56 (d), 207.32 (s).

**(3*R*,5*R*)-3,5-Bis[(*tert*-butyldimethylsilyloxy)-1,4-cyclohexanedione (11)**. To a stirred mixture of ruthenium(III) chloride hydrate (331 mg, 1.6 mmol) and sodium periodate (8.37 g, 39.2 mmol) in water (32 mL) was added a solution of hydroxy ketone **10** (4.05 g, 10.8 mmol) in CCl<sub>4</sub>/CH<sub>3</sub>CN (1:1, 48 mL). The mixture was vigorously stirred at room temperature for 22 h. A few drops of 2-propanol were added, and the mixture was poured into water and extracted with toluene. The organic layer was washed with 1% NaHSO<sub>3</sub> and brine, dried (MgSO<sub>4</sub>), and evaporated to give a dark oily residue which was purified by flash chromatography. Elution with hexane/ethyl acetate (9:1) gave pure, semicrystalline diketone **11** (2.04 g, 65% based on recovered hydroxy ketone **10**) and unchanged substrate (0.88 g). **11**:  $[\alpha]_D^{25} -40.2^\circ$  (*c* 0.5, CHCl<sub>3</sub>); <sup>1</sup>H NMR (CDCl<sub>3</sub>)  $\delta$  0.073 and 0.094 (each 6H, each s, 4  $\times$  SiCH<sub>3</sub>), 0.888 (18H, s, 2  $\times$  Si-*t*-Bu), 2.71 (2H, ddd, *J* = 15.0, 7.4, 1.9 Hz), 2.89 (2H, ddd, *J* = 15.0, 5.2, 1.9 Hz), 4.66 (2H, dd, *J* = 7.4, 5.2 Hz); <sup>13</sup>C NMR (CDCl<sub>3</sub>)  $\delta$  –5.22 (q), –4.94 (q), –4.81 (q), –4.74 (q), 18.01 (s), 18.15 (s), 25.59 (q), 25.69 (q), 46.89 (t), 49.55 (t), 71.79 (d), 72.05 (d), 203.18 (s), 206.12 (s); MS *m/z* (relative intensity) no M<sup>+</sup> 357 (M<sup>+</sup> – Me, 4), 315 (M<sup>+</sup> – *t*-Bu, 100), 297 (3), 271 (14), 183 (32), 73 (85).

**[(3*R*,5*R*)-3',5'-Bis[(*tert*-butyldimethylsilyloxy)-4'-oxocyclohexylidene]acetic Acid Methyl Ester (12)**. To a solution of diisopropylamine (0.44 mL, 3.14 mmol) in anhydrous THF (2.2 mL) was added *n*-BuLi (2.5 M in hexanes, 1.26 mL, 3.15 mmol) under argon at –78 °C; the mixture was stirred, and methyl(trimethylsilyl)acetate (0.52 mL, 3.17 mmol) was then added. After 15 min, the diketone **11** (819.8 mg, 2.2 mmol) in anhydrous THF (2.2 + 1 mL) was added dropwise over 8 min. The solution was stirred at –78 °C for an additional 12 min, and the reaction was quenched with wet ether. The mixture was poured into brine and extracted with ether and benzene. The combined extracts were washed with brine, dried (MgSO<sub>4</sub>), and evaporated. The light-brown oily residue was purified by flash chromatography. Elution with hexane/ethyl acetate (95:5) gave a pure allylic ester **12** (601.8 mg, 64%) as a colorless oil which slowly crystallized upon standing in the refrigerator.

**[(3*R*,5*R*)-3',5'-Bis[(*tert*-butyldimethylsilyloxy)-4'-ethylidenecyclohexylidene]acetic Acid Methyl Esters (13 and 14)**. To the ethyltriphenylphosphonium bromide (104 mg, 0.28 mmol) in anhydrous THF (1.3 mL) at 0 °C was added dropwise *n*-BuLi (1.6 M in hexanes, 0.18 mL, 0.29 mmol) under argon while the mixture was stirred; the solution was stirred at 0 °C for 10 min, and then at room temperature for 10 min. The orange-red mixture was cooled to –78 °C and siphoned in 3 equal portions (20 and 50 min intervals between the next portions) into a solution of ketoester **12** (24 mg, 56  $\mu$ mol) in anhydrous THF (0.5 mL) at –78 °C. The reaction mixture (yellow solution with colorless precipitate) was stirred at –78 °C, and the reaction was quenched by the addition of brine containing 1% HCl (3 h 40 min after addition of the first portion of the Wittig reagent), AcOEt (15 mL), benzene (10 mL), ether (5 mL), and saturated NaHCO<sub>3</sub> (10 mL) were added, and the mixture was vigorously stirred at room temperature for 18 h. The organic phase was separated,

washed with brine, dried (MgSO<sub>4</sub>), and evaporated. The residue was dissolved in hexane, applied on a silica Sep-Pak cartridge, and washed with hexane (20 mL) to remove apolar impurities. Elution with hexane/ethyl acetate (99.2:0.8, 20 mL) gave impure 4'-ethylidene compounds **13** and **14** as a colorless oil (ca. 8 mg). Purification of the products was achieved by HPLC (10 mm  $\times$  25 cm Zorbax-Sil column, 4 mL/min) using the hexane/ethyl acetate (98:2) solvent system. Pure compounds **13** and **14** were eluted at *R<sub>v</sub>* 34 mL (single peak) as a colorless oil (4.4 mg, 18%; **13**:**14** isomer ratio of 1:1.7).

**2-[(3*R*,5*R*)-3',5'-Bis[(*tert*-butyldimethylsilyloxy)-4'-ethylidenecyclohexylidene]ethanol (15 and 16)**. Diisobutylaluminum hydride (1.5 M in toluene, 0.2 mL, 0.3 mmol) was slowly added to a stirred solution of the allylic esters **13** and **14** (1:1.7, 29.6 mg, 67  $\mu$ mol) in toluene/methylene chloride (2:1, 1.2 mL) at –78 °C under argon. The mixture was stirred at –78 °C for 1 h; the reaction was quenched by the addition of potassium sodium tartrate (2 N, 1 mL), aq HCl (2 N, 1 mL), and H<sub>2</sub>O (12 mL), and then the mixture was diluted with ether and benzene. The organic layer was washed with diluted NaHCO<sub>3</sub> and brine, dried (MgSO<sub>4</sub>), and evaporated. The residue was purified by flash chromatography. Elution with hexane/ethyl acetate (95:5) gave semicrystalline allylic alcohols **15** and **16** (22.1 mg, 80%, **15**:**16** isomer ratio of 1:1.8). Separation of both isomers was achieved by HPLC (10 mm  $\times$  25 cm Zorbax-Sil column, 4 mL/min) using the hexane/ethyl acetate (9:1) solvent system. Pure compounds **15** (oily) and **16** (crystalline) were eluted at *R<sub>v</sub>* 44 and 47 mL, respectively.

**[2-[(3*R*,5*R*)-3',5'-Bis[(*tert*-butyldimethylsilyloxy)-4'-ethylidenecyclohexylidene]ethyl]diphenylphosphine Oxides (17 and 18)**. (1) To the allylic alcohols **15** and **16** (1:1.7, 21.7 mg, 53  $\mu$ mol) in anhydrous THF (0.5 mL) was added *n*-BuLi (2.5 M in hexanes, 21  $\mu$ L, 53  $\mu$ mol) under argon at 0 °C with stirring. Freshly recrystallized tosyl chloride (10.1 mg, 53  $\mu$ mol) was dissolved in anhydrous THF (100  $\mu$ L) and added to the allylic alcohol–BuLi solution. The mixture was stirred at 0 °C for 5 min and set aside. In another dry flask with air replaced by argon, *n*-BuLi (2.5 M in hexanes, 42  $\mu$ L, 105  $\mu$ mol) was added to Ph<sub>2</sub>PH (18  $\mu$ L, 100  $\mu$ mol) in anhydrous THF (150  $\mu$ L) at 0 °C while the mixture was stirred. The red solution was siphoned under argon pressure to the solution of tosylate until the orange color persisted (ca. one-half of the solution was added). The resulting mixture was stirred for an additional 30 min at 0 °C, and the reaction was quenched by the addition of H<sub>2</sub>O (10  $\mu$ L). Solvents were evaporated under reduced pressure, and the residue was dissolved in methylene chloride (0.5 mL) and stirred with 10% H<sub>2</sub>O<sub>2</sub> (0.25 mL) at 0 °C for 1 h. The organic layer was separated, washed with cold aq sodium sulfite and H<sub>2</sub>O, dried (MgSO<sub>4</sub>), and evaporated. The residue was subjected to flash chromatography. Elution with hexane/ethyl acetate (9:1) gave unchanged allylic alcohols (4.0 mg). Subsequent elution with benzene/ethyl acetate (7:3) provided a mixture of phosphine oxides **17** and **18** (14.7 mg, 46%, 56% based on recovered starting material). (2) Pure phosphine oxides **17** (60% yield) and **18** (56% yield) were prepared in the same way from the corresponding individual allylic alcohols **15** and **16**, respectively. Analytical samples of both isomers were obtained after HPLC (10 mm  $\times$  25 cm Zorbax-Sil column, 4 mL/min) using the hexane/2-propanol (9:1) solvent system. Pure compounds **17** (oily) and **18** (crystalline) were eluted at *R<sub>v</sub>* 37 and 39 mL, respectively.

**1 $\alpha$ -[(*tert*-Butyldimethylsilyloxy)-2-ethylidene-25-[(triethylsilyloxy)-19-norvitamin D<sub>3</sub> *tert*-Butyldimethylsilyloxy] Ether (20a and 21a)**. (1) To a solution of phosphine oxides **17** and **18** (1:1.7, 4.2 mg, 7.0  $\mu$ mol) in anhydrous THF (140  $\mu$ L) at –78 °C was slowly added phenyllithium (1.8 M in cyclohexane/ether, 4  $\mu$ L, 7.2  $\mu$ mol) under argon while the mixture was stirred. The solution turned deep orange. The mixture was stirred at –78 °C for 20 min, and a precooled (–78 °C) solution of protected hydroxy ketone **19a** (4.5 mg, 11.4  $\mu$ mol; prepared according to a published procedure<sup>9</sup>) in anhydrous THF (100 + 50  $\mu$ L) was slowly added. The mixture was stirred under argon at –78 °C for 3 h and at 0 °C for 19 h. Ethyl acetate and water were added, and the organic phase

was washed with brine, dried (MgSO<sub>4</sub>), and evaporated. The residue was dissolved in hexane, applied on a silica Sep-Pak cartridge, and washed with hexane/ethyl acetate (99.7:0.3, 20 mL) to give 19-norvitamin derivatives **20a** and **21a** (1.6 mg, 29%, 55% based on recovered substrates). The Sep-Pak was then washed with hexane/ethyl acetate (96:4, 10 mL) to recover some unchanged C,D-ring ketone **19a** (3 mg) and with ethyl acetate (10 mL) to recover diphenylphosphine oxide (2 mg). The mixture of protected vitamins was separated by HPLC (6.2 mm  $\times$  25 cm Zorbax-Sil column, 4 mL/min) using the hexane/ethyl acetate (99.95:0.05) solvent system. Pure compounds **20a** (1.4 mg) and **21a** (0.2 mg) were eluted at *R<sub>v</sub>* 29 and 36 mL, respectively, as colorless oils.

(2) When pure phosphine oxides **17** and **18** were used as substrates for Wittig–Horner coupling with **19a** (performed in a manner analogously to the procedure described above), the corresponding protected 19-norvitamin D<sub>3</sub> compounds **20a** and **21a** were obtained in 9 and 13% yield, respectively.

**(20S)-1 $\alpha$ -[(*tert*-Butyldimethylsilyloxy]-2-ethylidene-25-[(triethylsilyloxy)-19-norvitamin D<sub>3</sub> *tert*-Butyldimethylsilyl Ethers (**20b** and **21b**).** Protected 19-norvitamin D<sub>3</sub> compounds **20b** and **21b** were obtained by the Wittig–Horner reaction of the protected Grundmann's ketone **19b** (prepared according to a published procedure<sup>6</sup>) and the corresponding phosphine oxides **17** and **18**, performed as described for preparation of **20a** and **21a**. Separation of the crude products **20b** and **21b** was achieved by Sep-Pak filtration, and their final purification was performed by HPLC (10 mm  $\times$  25 cm Zorbax-Sil column, 4 mL/min) using the hexane/ethyl acetate (99.75:0.25) solvent system. Pure compounds **20b** and **21b** were eluted at *R<sub>v</sub>* 25 and 27 mL, respectively, as colorless oils (90 and 15% yield, respectively).

**1 $\alpha$ ,25-Dihydroxy-2-ethylidene-19-norvitamin D<sub>3</sub> (**8a** and **9a**).** The protected vitamin **20a** or **21a** (2.4 mg, 3  $\mu$ mol) in anhydrous THF (200  $\mu$ L) was treated with tetrabutylammonium fluoride (1.0 M in THF, 60  $\mu$ L, 60  $\mu$ mol). The mixture was stirred under argon at room temperature for 23 h, poured into brine, and extracted with ethyl acetate and ether. Organic extracts were washed with brine, dried (MgSO<sub>4</sub>), and evaporated. The residue was purified by HPLC (6.2 mm  $\times$  25 cm Zorbax-Sil column, 4 mL/min) using the hexane/2-propanol (9:1) solvent system. Analytically pure 2-ethylidene-19-norvitamin **8a** (0.86 mg, 64%) was collected at *R<sub>v</sub>* 25 mL, whereas the isomeric compound **9a** (0.75 mg, 56%) was eluted at *R<sub>v</sub>* 24 mL (1 $\alpha$ ,25-dihydroxyvitamin D<sub>3</sub> was eluted at *R<sub>v</sub>* 49 mL in the same system) as a white solid. Purity of both compounds **8a** and **9a** was confirmed by reversed-phase HPLC (6.2 mm  $\times$  25 cm Zorbax-ODS column, 2 mL/min) using the methanol/water (8:2) solvent system; they were eluted as single sharp peaks at *R<sub>v</sub>* 33 and 40 mL, respectively.

**(20S)-1 $\alpha$ ,25-Dihydroxy-2-ethylidene-19-norvitamin D<sub>3</sub> (**8b** and **9b**).** Vitamins **8b** and **9b** were prepared from the corresponding protected compounds **20b** and **21b** by treatment with tetrabutylammonium fluoride, performed as described for isomers **8a** and **9a** from the 20*R*-series. The products were purified by HPLC (6.2 mm  $\times$  25 cm Zorbax-Sil column, 4 mL/min) using the hexane/2-propanol (9:1) solvent system. Analytically pure 2-ethylidene-19-norvitamins **8b** (75% yield) and **9b** (61% yield) were collected at *R<sub>v</sub>* ca. 23 mL. Purity of both compounds **8b** and **9b** was confirmed by reversed-phase HPLC (6.2 mm  $\times$  25 cm Zorbax-ODS column, 2 mL/min) using the methanol/water (8:2) solvent system; they were eluted as single sharp peaks at *R<sub>v</sub>* 25 and 44 mL, respectively.

**1 $\alpha$ ,25-Dihydroxy-2 $\alpha$ - and 1 $\alpha$ ,25-Dihydroxy-2 $\beta$ -ethyl-19-norvitamin D<sub>3</sub> (**6a** and **7a**).** Tris(triphenylphosphine)rhodium(I) chloride (4.6 mg, 5  $\mu$ mol) was added to dry benzene (2.5 mL) presaturated with hydrogen. The mixture was stirred at room temperature until a homogeneous solution was formed (ca. 40 min). A solution of vitamin **8a** (1.1 mg, 2.6  $\mu$ mol) in dry benzene (0.5 mL) was then added, and the reaction was allowed to proceed under a continuous stream of hydrogen for 3.5 h. Another portion of catalyst (3.7 mg, 4  $\mu$ mol) was added, and the hydrogenation continued for the next 6 h. Benzene was removed under vacuum, and the residue was redissolved

in hexane/ethyl acetate (6:4, 2 mL) and applied on Waters silica Sep-Pak. A mixture of 2-ethyl vitamins was eluted with the same solvent system (20 mL). The compounds were further purified by HPLC (10 mm  $\times$  25 cm Zorbax-Sil column, 4 mL/min) using the hexane/2-propanol (85:15) solvent system. The mixture of 2-ethyl-19-norvitamins **6a** and **7a** (0.52 mg, 47%) gave a single peak at *R<sub>v</sub>* 28 mL, and unreacted substrate (20  $\mu$ g) was eluted at *R<sub>v</sub>* 35 mL. Separation of both epimeric products was achieved by reversed-phase HPLC (6.2 mm  $\times$  25 cm Zorbax-ODS column, 2 mL/min) using the methanol/water (8:2) solvent system. 2 $\beta$ -Ethyl vitamin **7a** (124  $\mu$ g, 11%) was collected at *R<sub>v</sub>* 37 mL and its 2 $\alpha$ -epimer **6a** (362  $\mu$ g, 33%) at *R<sub>v</sub>* 42 mL.

**(20S)-1 $\alpha$ ,25-Dihydroxy-2 $\alpha$ - and (20S)-1 $\alpha$ ,25-Dihydroxy-2 $\beta$ -ethyl-19-norvitamin D<sub>3</sub> (**6b** and **7b**).** Vitamins **6b** and **7b** were obtained by hydrogenation of **8b** and **9b**, performed in a manner analogous to the process described above for 20*R*-isomers **8a** and **9a**. The hydrogenated compounds were first purified by HPLC (10 mm  $\times$  25 cm Zorbax-Sil column, 4 mL/min) using the hexane/2-propanol (85:15) solvent system. The mixture of 2-ethyl-19-norvitamins **7b** and **6b** (ca. 45%) gave partially overlapped peaks at *R<sub>v</sub>* 27 and 29 mL, respectively. Separation of both epimers was easily achieved by reversed-phase HPLC (6.2 mm  $\times$  25 cm Zorbax-ODS column, 2 mL/min) using the methanol/water (8:2) solvent system. 2 $\beta$ -Ethyl vitamin **7b** was collected at *R<sub>v</sub>* 30 mL and its 2 $\alpha$ -epimer **6b** at *R<sub>v</sub>* 45 mL.

**Biological Studies. 1. Measurement of Intestinal Calcium Transport and Bone Calcium Mobilization.** Twenty-day-old weanling male rats from the low-vitamin D colony were purchased from the Sprague Dawley Co. (Indianapolis, IN) and fed the vitamin D-deficient diet<sup>44</sup> containing 0.47% calcium and 0.3% phosphorus for 1 week. They were then switched to the reduced calcium diet (0.02% Ca) for an additional 2 weeks. These animals had no detectable levels of 25-OH-D<sub>3</sub> or 1 $\alpha$ ,25-(OH)<sub>2</sub>D<sub>3</sub> in their plasma as measured by methods described previously.<sup>45</sup> For this first experiment, the indicated rats received a single intravenous dose of the indicated compound in 0.05 mL of ethanol (data not shown). In the other experiment, the rats were given the indicated doses of compounds in 0.1 mL of 1,2-propanediol/ethanol (95:5) by intraperitoneal injection each day for 7 days. In the first experiment, the rats were euthanized at various times after the dose (data not shown). In the second experiment, they were sacrificed 24 h after the last dose. The rats were sacrificed under ether anesthesia by decapitation; their blood and intestines were collected and used immediately to determine calcium transport activity and serum calcium concentration. Calcium was measured in the presence of 0.1% lanthanum chloride by means of a Perkin-Elmer atomic absorption spectrometer model 3110. Intestinal calcium transport was determined by the everted intestinal sac method using the proximal 10 cm of intestine as described earlier.<sup>44</sup> Statistical analysis was by the Student's *t* test.<sup>46</sup> Intestinal calcium transport is expressed as the serosal/mucosal ratio of calcium in the sac to the calcium in the final incubation medium or S/M. Bone calcium mobilization represents the rise in serum calcium of the rats maintained on a very low-calcium diet. In that measurement, the increase in serum calcium must arise from bone and, hence, is a determination of bone calcium mobilization.

**2. Measurement of Cellular Differentiation.** Human leukemia HL-60 cells (obtained from ATTC) were plated at 2  $\times$  10<sup>5</sup> cells per plate and incubated in Eagle's modified medium as described previously.<sup>4c</sup> The compounds tested were added in the indicated concentrations in 0.05 mL of ethanol so that the ethanol concentration never exceeded 1%. The incubation was carried out for 4 days, and at the end of the fourth day, superoxide production was measured by nitro blue tetrazolium (NBT) reduction. The number of cells containing intracellular black-blue formazan deposits was determined by light microscopy using a hemacytometer. At least 200 cells were counted in duplicate per determination. Percentage differentiation represents the percentage of cells providing NBT reduction appearance. The results were plotted on semilog paper, and

relative differentiation activities of the analogues were determined by comparison of the compound concentrations capable of inducing 50% maturation according to the assay. This method is described in detail elsewhere.<sup>4c</sup> The experiment was repeated 3 times, and the results are reported as the mean  $\pm$  SD.

**3. Measurement of Binding to the Porcine Intestinal Vitamin D Receptor.** Porcine intestinal nuclear extract was prepared as described earlier.<sup>47</sup> It was diluted, and 0.1 mg of protein (200 fmol of binding activity) in 100  $\mu$ L was used in each tube.  $1\alpha,25\text{-(OH)}_2[26,27\text{-}^3\text{H}]\text{D}_3$  (10 000 cpm) was added in 2.0  $\mu$ L of ethanol. To this mixture was added either standard radioinert  $1\alpha,25\text{-(OH)}_2\text{D}_3$  at various concentrations or the indicated analogue at various concentrations in 5  $\mu$ L of ethanol. The mixture was incubated at room temperature for 4 h on a shaker, and then 100  $\mu$ L of hydroxyapatite (50% slurry) was added. The sample was vortexed at 5 min intervals for a total of 15 min on ice. The hydroxyapatite was then washed 3 times by adding 0.5 mL of TE 5% Triton X-100, centrifuging at 200g for 5 min, and aspirating the supernatant. The radioactivity bound to the hydroxyapatite was determined by liquid scintillation counting in Bio-Safe II scintillation fluid. The values are plotted versus concentration of analogue or standard. Each value represents triplicate values. The displacement experiments were carried out in triplicate on two different occasions.

**Molecular Modeling. 1. Modeling of the VDR Three-Dimensional Structure.** The computations in this work involve several steps. In the crucial one, we employed lattice modeling (SICHO method) to generate the full-length model of the ligand binding domain of the vitamin D receptor. Homologous parts of the receptor (residues 118–163 and 207–423) were built using the crystal structure of the hVDR truncated mutant (118–425,  $\Delta[165\text{--}215]$ ) as the template for traditional comparative modeling. Such a model is lacking the highly nonhomologous insertion domain of the protein (encompassing residues 164–207). It is well-known that such big gaps in protein structures cannot be reasonably filled by using conventional comparative modeling tools.<sup>34,35,49</sup> It is also impractical (due to the extreme computational cost) to assemble these large protein fragments by means of standard molecular dynamics simulations. For these reasons, we employed the recently developed lattice model for protein folding and distant homology modeling.<sup>35</sup> This method used the simplified SICHO protein models and a set of statistical potentials for efficient searching of protein conformational space. The SICHO model enables simulations of the entire folding process of small proteins, large-scale relaxation of poor-quality models originated from sparse alignments (or threading alignments), and “docking” of relatively large protein fragments to the partially determined protein structures.<sup>49</sup> The last is exactly the case of the present application. Thus, in the first stage, we built the homologous part of the structure using rather standard procedures described previously.<sup>34</sup> The crystal structure of the holo hVDR deletion mutant (118–425,  $\Delta[165\text{--}215]$ ) was employed as a template for comparative modeling of this well-defined part of the structure. The nonhomologous part (residues 165–207) of the full-length model (residues 118–423) of rVDR-LBD was assembled on the scaffold of this incomplete structure. The procedure worked as follows: a random loop that connects the two parts of the structure was constructed. Optimization (or folding) of this part of the molecule was done using a reduced lattice representation, knowledge-based force field of the SICHO model, and Monte Carlo sampling technique. The procedure was repeated several times, and the lowest-energy conformation of the loop was finally subject to reconstruction of the all-atom structure using the lattice skeleton of the loop as a template.

It is important to mention that the accuracy of the SICHO method is within a range of 2–3 Å. Therefore, the overall pattern of side chain contacts between the variable loop and the rest of the molecule should be reproduced correctly; however, the atomic details (after all-atom reconstructions) are of low fidelity.

**2. Docking of Analogues to the Ligand Binding Pocket of the VDR.** Docking simulations of four analogues (**6a–9a**), whose synthesis is described in this work, were performed by FlexiDock software from TRIPOS<sup>50</sup> which employs genetic algorithms for the search of conformational space of the ligand with respect to the given structure of the receptor's binding site. Because FlexiDock requires an approximate starting position of the ligand to be provided, the docking procedures were carried out several times for each analogue, starting from arbitrarily chosen emplacement of the ligand with respect to the binding pocket of the receptor. Internal rotations around the single bonds (ring OH groups and side chain) of the ligands were allowed during the simulations. Several simulations (of 50 000 steps each) were performed with different initial positioning of the compound in the vicinity of the pocket and converged to approximately the same structure within the binding site. For final consideration, the structures of the lowest conformational energy of the ligand–receptor complex were selected.

Coordinates of the molecular models discussed in this work can be found on our home page (<http://biocomp.chem.uw.edu.pl>).

**Acknowledgment.** The authors are grateful for the generous amount of computer time granted to them by the Interdisciplinary Center for Mathematical and Computational Modeling of Warsaw University (ICM). We acknowledge the assistance of Rowland Randall in recording the mass spectra. The work was supported in part by funds from the Wisconsin Alumni Research Foundation and the National Foundation for Cancer Research.

**Supporting Information Available:** Purity criteria for target vitamin D compounds; spectral data of the synthesized compounds **6a,b–9a,b**, **12–18**, and **20a,b–21a,b**; and figures with either the competitive binding curves or dose–response curves derived from the cellular differentiation assay of the vitamin D analogues **6a,b–9a,b**. This material is available free of charge via the Internet at <http://pubs.acs.org>.

## References

- (1) DeLuca, H. F.; Burmester, J.; Darwish, H.; Krisinger, J. Molecular mechanism of the action of  $1,25\text{-dihydroxyvitamin D}_3$ . In *Comprehensive Medicinal Chemistry*; Hansch, C., Sammes, P. G., Taylor, J. B., Eds.; Pergamon Press: Oxford, 1991; Vol. 3, pp 1129–1143.
- (2) *Vitamin D, a pluripotent steroid hormone: Structural studies, molecular endocrinology and clinical applications*; Norman, A. W., Bouillon, R., Thomasset, M., Eds.; Walter de Gruyter: Berlin, 1994.
- (3) (a) DeLuca, H. F. Mechanisms and functions of vitamin D. *Nutr. Rev.* **1998**, *56*, S4–S10. (b) Reichel, H.; Koeffler, H. P.; Norman, A. W. The role of the vitamin D endocrine system in health and disease. *N. Engl. J. Med.* **1989**, *320*, 980–991. (c) DeLuca, H. F. The vitamin D story: A collaborative effort of basic science and clinical medicine. *FASEB J.* **1988**, *2*, 224–236. (d) Ikekawa, N. Structures and biological activities of vitamin D metabolites and their analogs. *Med. Res. Rev.* **1987**, *7*, 333–366. (e) DeLuca, H. F.; Schnoes, H. K. Vitamin D: Recent advances. *Annu. Rev. Biochem.* **1983**, *53*, 411–439.
- (4) (a) Jones, G.; Strugnell, S. A.; DeLuca, H. F. Current understanding of the molecular action of vitamin D. *Physiol. Rev.* **1998**, *78*, 1193–1231. (b) Suda, T. The role of  $1\alpha,25\text{-dihydroxyvitamin D}_3$  in the myeloid cell differentiation. *Proc. Soc. Exp. Biol. Med.* **1989**, *191*, 214–220. (c) Ostrem, V. K.; Lau, W. F.; Lee, S. H.; Perlman, K.; Prah, J.; Schnoes, H. K.; DeLuca, H. F.; Ikekawa, N. Induction of monocytic differentiation of HL-60 cells by  $1,25\text{-dihydroxyvitamin D}$  analogs. *J. Biol. Chem.* **1987**, *262*, 14164–14171. (d) Tsoukas, C. D.; Provvedini, D. M.; Manolagas, S. C.  $1,25\text{-Dihydroxyvitamin D}_3$ : A novel immunoregulatory hormone. *Science* **1984**, *224*, 1438–1440. (e) Mangelsdorf, D. J.; Koeffler, H. P.; Donaldson, C. A.; Pike, J. W.; Haussler, M. R.  $1\alpha,25\text{-Dihydroxyvitamin D}_3$ -induced differentiation in a human promyelocytic leukemia cell line (HL-60): Receptor mediated maturation of macrophage-like cells. *J. Cell Biol.* **1984**, *98*, 391–398. (f) Abe, E.; Miyaura, C.; Sakagami, H.; Takeda, M.; Konno, K.; Yamazaki, T.; Yoshiki, S.; Suda, T. Differentiation of mouse myeloid leukemia cells induced by  $1\alpha,25\text{-dihydroxyvitamin D}_3$ . *Proc. Natl. Acad. Sci. U.S.A.* **1981**, *78*, 4990–4994.

- (5) (a) Bouillon, R.; Okamura, W. H.; Norman, A. W. Structure–function relationship in the vitamin D endocrine system. *Endocr. Rev.* **1995**, *16*, 200–257. (b) Ikekawa, N. Structures and biological activities of vitamin D metabolites and their analogs. *Med. Res. Rev.* **1987**, *7*, 333–336. (c) DeLuca, H. F.; Paaren, H. E.; Schnoes, H. K. Vitamin D and calcium metabolism. *Top. Curr. Chem.* **1979**, *83*, 1–65. (d) Nishii, Y.; Okano, E. History of the development of new vitamin D analogs: studies on 2 $\alpha$ -oxacalcitriol (OCT) and 2 $\beta$ -(3-hydroxypropoxy)calcitriol (ED-71). *Steroids* **2001**, *66*, 137–146.
- (6) Sicinski, R. R.; Prah, J. M.; Smith, C. M.; DeLuca, H. F. New 1 $\alpha$ ,25-dihydroxy-19-norvitamin D<sub>3</sub> compounds of high biological activity: Synthesis and biological evaluation of 2-hydroxymethyl, 2-methyl, and 2-methylene analogues. *J. Med. Chem.* **1998**, *41*, 4662–4674.
- (7) (a) Perlman, K. L.; Swenson, R. E.; Paaren, H. E.; Schnoes, H. K.; DeLuca, H. F. Novel synthesis of 19-nor-vitamin D compounds. *Tetrahedron Lett.* **1991**, *32*, 7663–7666. (b) Perlman, K. L.; Sicinski, R. R.; Schnoes, H. K.; DeLuca, H. F. 1 $\alpha$ ,25-Dihydroxy-19-nor-vitamin D<sub>3</sub>, a novel synthetic vitamin D-related compound with potential therapeutic activity. *Tetrahedron Lett.* **1990**, *31*, 1823–1824.
- (8) (a) Lythgoe, B. Synthetic approaches to vitamin D and its relatives. *Chem. Soc. Rev.* **1981**, 449–475. (b) Lythgoe, B.; Moran, T. A.; Nambudiry, M. E. N.; Ruston, S. Allylic phosphine oxides as precursors of conjugated dienes of defined geometry. *J. Chem. Soc., Perkin Trans. 1* **1976**, 2386–2390.
- (9) Sicinski, R. R.; Perlman, K. L.; DeLuca, H. F. Synthesis and biological activity of 2-hydroxy and 2-alkoxy analogs of 1 $\alpha$ ,25-dihydroxy-19-norvitamin D<sub>3</sub>. *J. Med. Chem.* **1994**, *37*, 3730–3738.
- (10) DeLuca, H. F.; Schnoes, H. K.; Perlman, K. L.; Sicinski, R. R.; Prah, J. M. 19-Norvitamin D compounds. *Eur. Pat. Appl. EP 387,077; Chem. Abstr.* **1991**, *144*, 185853u.
- (11) Buss, A. D.; Warren, S. Stereocontrolled Horner–Wittig reactions: synthesis of disubstituted alkenes. *J. Chem. Soc., Perkin Trans. 1* **1985**, 2307–2325 and references therein.
- (12) (a) Clough, J. M.; Pattenden, G. Stereocontrolled synthesis of the di-*cis*-pentaene chromophore found in phytofluene from tangerine tomato fruits. *Tetrahedron Lett.* **1979**, *52*, 5043–5046. (b) Clough, J. M.; Pattenden, G. The synthesis of polyene isoprenoids by the Horner variant of the Wittig reaction. *Tetrahedron Lett.* **1978**, *43*, 4159–4162.
- (13) (a) Eguchi, T.; Ikekawa, N. Conformational analysis of 1 $\alpha$ ,25-dihydroxyvitamin D<sub>3</sub> by nuclear magnetic resonance. *Bioorg. Chem.* **1990**, *18*, 19–29. (b) Helmer, B.; Schnoes, H. K.; DeLuca, H. F. <sup>1</sup>H nuclear magnetic resonance studies of the conformations of vitamin D compounds in various solvents. *Arch. Biochem. Biophys.* **1985**, *241*, 608–615. (c) Wing, R. M.; Okamura, W. H.; Rego, A.; Pirió, M. R.; Norman, A. W. Studies on vitamin D and its analogs. VII. Solution conformations of vitamin D<sub>3</sub> and 1 $\alpha$ ,25-dihydroxyvitamin D<sub>3</sub> by high-resolution proton magnetic resonance spectroscopy. *J. Am. Chem. Soc.* **1975**, *97*, 4980–4985.
- (14) Some representative papers: (a) Ishida, H.; Shimizu, M.; Yamamoto, K.; Iwasaki, Y.; Yamada, S. Syntheses of 1-alkyl-1,25-dihydroxyvitamin D<sub>3</sub>. *J. Org. Chem.* **1995**, *60*, 1828–1833. (b) Berman, E.; Friedman, N.; Mazur, Y.; Sheves, M. Conformational equilibria in vitamin D. Synthesis and <sup>1</sup>H and <sup>13</sup>C dynamic nuclear magnetic resonance study of 4,4-dimethylvitamin D<sub>3</sub>, 4,4-dimethyl-1 $\alpha$ -hydroxyvitamin D<sub>3</sub>, and 4,4-dimethyl-1 $\alpha$ -hydroxyepivitamin D<sub>3</sub>. *J. Am. Chem. Soc.* **1978**, *100*, 5626–5634. (c) Okamura, W. H.; Mitra, M. N.; Pirió, M. R.; Mourino, A.; Carey, S. C.; Norman, A. W. Studies on vitamin D (calciferol) and its analogues. 13. 3-Deoxy-3 $\alpha$ -methyl-1 $\alpha$ -hydroxyvitamin D<sub>3</sub>, 3-deoxy-3 $\alpha$ -methyl-1 $\alpha$ ,25-dihydroxyvitamin D<sub>3</sub>, and 1 $\alpha$ -hydroxy-3-epivitamin D<sub>3</sub>. Analogues with conformationally biased A rings. *J. Org. Chem.* **1978**, *43*, 574–580. (d) Sheves, M.; Friedman, N.; Mazur, Y. Conformational equilibria in vitamin D. Synthesis of 1 $\beta$ -hydroxyvitamin D<sub>3</sub>. *J. Org. Chem.* **1977**, *42*, 3597–3599. (e) Berman, E.; Luz, Z.; Mazur, Y.; Sheves, M. Conformational analysis of vitamin D and analogues. <sup>13</sup>C and <sup>1</sup>H nuclear magnetic resonance study. *J. Org. Chem.* **1977**, *42*, 3325–3330.
- (15) Okamura, W. H.; Midland, M. M.; Hammond, M. W.; Abd. Rahman, N.; Dormanen, M. C.; Nemere, I.; Norman, A. W. Chemistry and conformation of vitamin D molecules. *J. Steroid Biochem. Mol. Biol.* **1995**, *53*, 603–613.
- (16) (a) Suhara, Y.; Nihei, K.-I.; Kurihara, M.; Kittaka, A.; Yamaguchi, K.; Fujishima, T.; Konno, K.; Miyata, N.; Takayama, H. Efficient and versatile synthesis of novel 2 $\alpha$ -substituted 1 $\alpha$ ,25-dihydroxyvitamin D<sub>3</sub> analogues and their docking to vitamin D receptors. *J. Org. Chem.* **2001**, *66*, 8760–8771. (b) Takayama, H.; Konno, K.; Fujishima, T.; Maki, S.; Liu, Z.; Miura, D.; Chokki, M.; Ishizuka, S.; Smith, C.; DeLuca, H. F.; Nakagawa, K.; Kurobe, M.; Okano, T. Systematic studies on synthesis, structural elucidation, and biological evaluation of A-ring diastereomers of 2-methyl-1 $\alpha$ ,25-dihydroxyvitamin D<sub>3</sub> and 20-epi-2-methyl-1 $\alpha$ ,25-dihydroxyvitamin D<sub>3</sub>. *Steroids* **2001**, *66*, 277–285.
- (c) Konno, K.; Fujishima, T.; Maki, S.; Liu, Z. P.; Miura, D.; Chokki, M.; Ishizuka, S.; Yamaguchi, K.; Kan, Y.; Kurihara, M.; Miyata, N.; Smith, C.; DeLuca, H. F.; Takayama, H. Synthesis, biological evaluation, and conformational analysis of A-ring diastereomers of 2-methyl-1 $\alpha$ ,25-dihydroxyvitamin D<sub>3</sub> and their 20-epimers: unique activity profiles depending on the stereochemistry of the A-ring and at C-20. *J. Med. Chem.* **2000**, *43*, 4247–4265. (d) Konno, K.; Maki, S.; Fujishima, T.; Liu, Z.; Miura, D.; Chokki, M.; Takayama, H. A novel and practical route to A-ring enyne synthon for 1 $\alpha$ ,25-dihydroxyvitamin D<sub>3</sub> analogs: Synthesis of A-ring diastereomers of 1 $\alpha$ ,25-dihydroxyvitamin D<sub>3</sub> and 2-methyl-1 $\alpha$ ,25-dihydroxyvitamin D<sub>3</sub>. *Bioorg. Med. Chem. Lett.* **1998**, *8*, 151–156. (e) Fujishima, T.; Liu, Z.-P.; Miura, D.; Chokki, M.; Ishizuka, S.; Konno, K.; Takayama, H. Synthesis and biological activity of 2-methyl-20-epi analogues of 1 $\alpha$ ,25-dihydroxyvitamin D<sub>3</sub>. *Bioorg. Med. Chem. Lett.* **1998**, *8*, 2145–2148.
- (17) Hirsch, J. A. Table of conformational energies-1967. *Top. Stereochem.* **1967**, *1*, 199–222.
- (18) (a) Johnson, F. Allylic strain in six-membered rings. *Chem. Rev.* **1968**, *68*, 375–413. (b) Johnson, F.; Malhotra, S. K. Steric interference in allylic and pseudo-allylic systems. I. Two stereochemical theorems. *J. Am. Chem. Soc.* **1965**, *87*, 5492–5493.
- (19) Nasipuri, D. *Stereochemistry of organic compounds*; Wiley Eastern: New Delhi, 1991; pp 270–271.
- (20) The calculation of optimized geometries and steric energies (*E*<sub>s</sub>) was carried out using the PC MODEL (release 6.0) software package (Serena Software, Bloomington, IN). Molecular modeling was performed in the MMX mode; the force field MMX is an enhanced version of MM2, with the pi-VESCF routines taken from MMP1.
- (21) Anet, F. A. L. The use of remote deuteration for the determination of coupling constants and conformational equilibria in cyclohexane derivatives. *J. Am. Chem. Soc.* **1962**, *84*, 1053–1054.
- (22) Okamura, W. H.; Norman, A. W.; Wing, R. M. Vitamin D: Concerning the relationship between molecular topology and biological function. *Proc. Natl. Acad. Sci. U.S.A.* **1974**, *71*, 4194–4197.
- (23) Sicinski, R. R.; DeLuca, H. F. Synthesis, conformational analysis, and biological activity of the 1 $\alpha$ ,25-dihydroxy-10,19-dihydrovitamin D<sub>3</sub> isomers. *Bioorg. Chem.* **1994**, *22*, 150–171.
- (24) Derivatives of 1 $\beta$ ,25-(OH)<sub>2</sub>D<sub>3</sub> substituted at C-2 with alkyls possessing terminal ( $\omega$ ) hydroxy or fluoro groups were also synthesized; some of them show interesting biological activities: (a) Posner, G. H.; Cho, C.-G.; Anjeh, T. E. N.; Johnson, N.; Horst, R. L.; Kobayashi, T.; Okano, T.; Tsugawa, N. 2-Fluoro-alkyl A-ring analogs of 1,25-dihydroxyvitamin D<sub>3</sub>. Stereocontrolled total synthesis via intramolecular and intermolecular Diels–Alder cycloadditions. Preliminary biological testing. *J. Org. Chem.* **1995**, *60*, 4617–4628. (b) Posner, G. H.; Johnson, N. Stereocontrolled total synthesis of calcitriol derivatives: 1,25-dihydroxy-2-(4'-hydroxybutyl)vitamin D<sub>3</sub> analogs of an osteoporosis drug. *J. Org. Chem.* **1994**, *59*, 7855–7861.
- (25) Rochel, N.; Wurtz, J. M.; Mitschler, A.; Klaholz, B.; Moras, D. The crystal structure of the nuclear receptor for vitamin D bound to its natural ligand. *Mol. Cell* **2000**, *5*, 173–179.
- (26) (a) Tocchini-Valentini, G. D.; Rochel, N.; Wurtz, J. M.; Mitschler, A.; Moras, D. Crystal structures of the vitamin D receptor complexed to superagonist 20-epi ligands. *Proc. Natl. Acad. Sci. U.S.A.* **2001**, *98*, 5491–5496. (b) Tocchini-Valentini, G. D.; Rochel, N.; Mitschler, A.; Moras, D. Ligand binding to the nuclear receptor for vitamin D. In *Vitamin D endocrine system: Structural, biological, genetic and clinical aspects*; Norman, A. W., Bouillon, R., Thomasset, M., Eds.; University of California–Riverside: Riverside, CA, 2000; pp 207–214.
- (27) Maenpaa, P. H.; Vaisanen, S.; Jaaskelainen, T.; Ryhanen, S.; Rouvinen, R.; Duchier, C.; Mahonen, A. Vitamin D<sub>3</sub> analogs (MC 1288, KH 1060, EB 1089, GS 1558, and CB 1093): Studies on their mechanism of action. *Steroids* **2001**, *66*, 223–225.
- (28) Liu, Y. Y.; Collins, E. D.; Norman, A. W.; Peleg, S. Differential interaction of 1 $\alpha$ ,25-dihydroxyvitamin D<sub>3</sub> analogues and their 20-epi homologues with the vitamin D receptor. *J. Biol. Chem.* **1997**, *272*, 3336–3345.
- (29) Yamamoto, K.; Masuno, H.; Choi, M.; Nakashima, K.; Taga, T.; Oozumi, H.; Umesono, K.; Sicinska, W.; VanHooke, J.; DeLuca, H. F.; Yamada, S. Three-dimensional modeling of and ligand docking to vitamin D receptor ligand binding domain. *Proc. Natl. Acad. Sci. U.S.A.* **2000**, *97*, 1467–1472.
- (30) Evans, R. M. The steroid and thyroid hormone receptor superfamily. *Science* **1988**, *240*, 889–895.
- (31) Wurtz, J. M.; Bourguet, W.; Renaud, J. P.; Vivat, V.; Chambon, P.; Moras, D.; Gronemeyer, H. A canonical structure for the ligand binding domain of nuclear receptors. *Nat. Struct. Biol.* **1996**, *3*, 87–94.
- (32) (a) Brown, T. A.; DeLuca, H. F. Sites of phosphorylation and photoaffinity labeling of the 1 $\alpha$ ,25-dihydroxyvitamin D<sub>3</sub> receptor. *Arch. Biochem. Biophys.* **1991**, *286*, 466–472. (b) Jurutka, P. W.;

- Hsieh, J. C.; Nakajima, S.; Haussler, C. A.; Whitfield, G. K.; Haussler, M. R. Human vitamin D receptor phosphorylation by casein kinase II at Ser-208 potentiates transcriptional activation. *Proc. Natl. Acad. Sci. U.S.A.* **1996**, *93*, 3519–3524.
- (33) Swamy, N.; Xu, W.; Paz, N.; Hsieh, J.-Ch.; Haussler, M. P.; Maalouf, G. J.; Mohr, S. C.; Ray, R. Molecular modeling, affinity labeling, and site-directed mutagenesis define the key points of interaction between the ligand-binding domain of the vitamin D nuclear receptor and  $1\alpha,25$ -dihydroxyvitamin D<sub>3</sub>. *Biochemistry* **2000**, *39*, 12162–12171.
- (34) Rotkiewicz, P.; Sicinska, W.; Kolinski, A.; DeLuca, H. F. Model of three-dimensional structure of vitamin D receptor and its binding mechanism with  $1\alpha,25$ -dihydroxyvitamin D<sub>3</sub>. *Proteins: Struct., Funct., Genet.* **2001**, *44*, 188–199.
- (35) (a) Kolinski, A.; Rotkiewicz, P.; Ilkowski, B.; Skolnick, J. Protein folding: flexible lattice models. *Prog. Theor. Phys.* **2000**, *138*, 292–302. (b) Kolinski, A.; Rotkiewicz, P.; Ilkowski, B.; Skolnick, J. A method for the improvement of the threading-based protein models. *Proteins* **1999**, *37*, 592–610. (c) Kolinski, A.; Skolnick, J. Assembly of protein structure from sparse experimental data: an efficient Monte Carlo model. *Proteins* **1998**, *32*, 476–474.
- (36) Rochel, N.; Tocchini-Valentini, G.; Egea, P. F.; Juntunen, K.; Garnier, J.-M.; Vihko, P.; Moras, D. Functional and structural characterization of the insertion region in the ligand binding domain of the vitamin D nuclear receptor. *Eur. J. Biochem.* **2001**, *268*, 971–979.
- (37) (a) Malloy, P. J.; Pike, J. W.; Feldman, D. The vitamin D receptor and the syndrome of hereditary  $1,25$ -dihydroxyvitamin D-resistant rickets. *Endocr. Rev.* **1999**, *20*, 156–188. (b) Vaisanen, S.; Juntunen, K.; Itkonen, A.; Vihko, P.; Maenpaa, P. Conformational studies of human vitamin-D receptor by antipeptide antibodies, partial proteolytic digestion and ligand binding. *Eur. J. Biochem.* **1997**, *248*, 156–162.
- (38) Gerstein, M.; Levitt, M. Using Iterative Dynamic Programming to Obtain Accurate Pairwise and Multiple Alignments of Protein Structures. *Proc. ISMB-96* **1996**, 59–67.
- (39) (a) Swamy, N.; Paz, N.; Mohr, S. C.; Xu, W.; Hsieh, J. C.; Ray, R. Three-dimensional architecture of the vitamin D receptor-ligand binding domain by affinity labeling, point-mutagenesis and homology modeling. *J. Bone Miner. Res.* Program of 21st Annual Meeting of ASBMR, **1999**, *14* (Suppl. 1), S303, F466. (b) Swamy, N.; Kounine, M.; Ray, R. Identification of the subdomain in the nuclear receptor for the hormonal form of the vitamin D<sub>3</sub>,  $1\alpha,25$ -dihydroxyvitamin D<sub>3</sub>, vitamin D receptor, that is covalently modified by an affinity labeling reagent. *Arch. Biochem. Biophys.* **1997**, *348*, 91–95.
- (40) Ray, R.; Swamy, N.; MacDonald, P. N.; Ray, S.; Haussler, M. R.; Holick, M. F. Affinity labeling of the  $1\alpha,25$ -dihydroxyvitamin D<sub>3</sub> receptor. *J. Biol. Chem.* **1996**, *271*, 2012–2017.
- (41) Fujishima, T.; Konno, K.; Nakagawa, K.; Tanaka, M.; Okano, T.; Kurihara, M.; Miyata, N.; Takayama, H. Synthesis and biological evaluation of all A-ring stereoisomers of 5,6-*trans*-2-methyl- $1,25$ -dihydroxyvitamin D<sub>3</sub> and their 20-epimers: possible binding modes of potent A-ring analogues to vitamin D receptor. *Chem. Biol.* **2001**, *8*, 1011–1024.
- (42) Liu, Y.-Y.; Nguyen, C.; Peleg, S. Regulation of ligand-induced heterodimerization and coactivator interaction by the activation function-2 domain of the vitamin D receptor. *Mol. Endocrinol.* **2000**, *14*, 1776–1787.
- (43) Siu-Caldera, M.-L.; Rao, D. S.; Astecker, N.; Weiskopf, A.; Vouros, P.; Konno, K.; Fujishima, T.; Takayama, H.; Peleg, S.; Reddy, G. S. Tissue specific metabolism of  $1\alpha,25$ -dihydroxy-20-epi-vitamin D<sub>3</sub> into new metabolites with significant biological activity: studies in rat osteosarcoma cells (UMR 106 and ROS 17/2.8). *J. Cell. Biochem.* **2001**, *82*, 599–609.
- (44) Suda, T.; DeLuca, H. F.; Tanaka, Y. Biological activity of 25-hydroxyergocalciferol in rats. *J. Nutr.* **1970**, *100*, 1049–1052.
- (45) Uhland-Smith, A.; DeLuca, H. F.  $1,25$ -Dihydroxycholecalciferol analogs cannot replace vitamin D in normocalcemic male rats. *J. Nutr.* **1993**, *123*, 1777–1785.
- (46) Snedecor, G. W.; Cochran, W. G. *Statistical Methods*, 6th ed.; Iowa State University Press: Ames, IA, 1967.
- (47) Dame, M. C.; Pierce, E. A.; Prahl, J. M.; Hayes, C. E.; DeLuca, H. F. Monoclonal antibodies to the porcine intestinal receptor for  $1,25$ -dihydroxyvitamin D<sub>3</sub>: Interaction with distinct receptor domains. *Biochemistry* **1986**, *25*, 4523–4534.
- (48) Wurtz, J. M.; Guillot, B.; Moras, D. 3D model of ligand binding domain of the vitamin D nuclear receptor based on the crystal structure of holo RAR- $\gamma$ . In *Vitamin D: Chemistry, biology and clinical applications of the steroid hormone*; Norman, A. W., Bouillon, R., Thomasset, M., Eds.; University of California–Riverside: Riverside, CA, 1997; pp 165–172.
- (49) Kolinski, A.; Rotkiewicz, P.; Skolnick, J. Structure of proteins: New approach to molecular modeling. *Pol. J. Chem.* **2001**, *75*, 587–599.
- (50) SYBYL, version 6.5; Tripos Inc.: St. Louis, MO.

JM020007M